

Developmental Transcriptome of *Aplysia californica*

ANDREAS HEYLAND^{1*}, ZER VUE², CHRISTIAN R. VOOLSTRA^{2,3},
MÓNICA MEDINA², AND LEONID L. MOROZ^{4,5*}

¹Integrative Biology, University of Guelph, Ontario, Canada

²University of California, Merced, School of Natural Sciences, Merced, California

³Red Sea Research Center, King Abdullah University of Science and Technology (KAUST), Thuwal, Saudi Arabia

⁴The Whitney Laboratory for Marine Bioscience, University of Florida, Florida

⁵Department of Neuroscience, University of Florida, Florida



ABSTRACT

Genome-wide transcriptional changes in development provide important insight into mechanisms underlying growth, differentiation, and patterning. However, such large-scale developmental studies have been limited to a few representatives of Ecdysozoans and Chordates. Here, we characterize transcriptomes of embryonic, larval, and metamorphic development in the marine mollusc *Aplysia californica* and reveal novel molecular components associated with life history transitions. Specifically, we identify more than 20 signal peptides, putative hormones, and transcription factors in association with early development and metamorphic stages—many of which seem to be evolutionarily conserved elements of signal transduction pathways. We also characterize genes related to biomineralization—a critical process of molluscan development. In summary, our experiment provides the first large-scale survey of gene expression in mollusc development, and complements previous studies on the regulatory mechanisms underlying body plan patterning and the formation of larval and juvenile structures. This study serves as a resource for further functional annotation of transcripts and genes in *Aplysia*, specifically and molluscs in general. A comparison of the *Aplysia* developmental transcriptome with similar studies in the zebra fish *Danio rerio*, the fruit fly *Drosophila melanogaster*, the nematode *Caenorhabditis elegans*, and other studies on molluscs suggests an overall highly divergent pattern of gene regulatory mechanisms that are likely a consequence of the different developmental modes of these organisms. *J. Exp. Zool. (Mol. Dev. Evol.)* 316:113–134, 2011. © 2010 Wiley-Liss, Inc.

J. Exp. Zool.
(*Mol. Dev. Evol.*)
316:113–134, 2011

How to cite this article: Heyland A, Vue Z, Voolstra CR, Medina M, Moroz LL. 2011. Developmental transcriptome of *Aplysia californica*. *J. Exp. Zool. (Mol. Dev. Evol.)* 316:113–134.

Identification of spatial and temporal dynamics of patterns of gene expression during development provides important insights into mechanisms linking phenotypes with genotypes. A detailed understanding of the regulatory machinery underlying gene expression (i.e. *cis* and *trans* regulation) is essential to address fundamental questions about the genomic basis of complex developmental programs (e.g. see Davidson, 2001; Wilkins, 2001; Rifkin et al., 2003). Major insights into these mechanisms originate primarily from representatives of the Deuterostomata and Ecdysozoa, and limited information exists on genome-wide changes in gene expression patterns for the Lophotrochozoa (but see Williams et al., 2009; Fiedler et al., 2010). Still, the

Grant Sponsors: Swiss National Science Foundation Stipendium fuer Angehende Forscher, Brain Research Foundation; NSERC; Grant number: C400230; Grant Sponsor: CFI; Grant number: 460175; Grant Sponsor: NIH; Grant numbers: P50HG002806; R01NS06076; RR025699; Grant Sponsor: NSF; Grant numbers: 0744649; DEB-0542330.

Additional Supporting Information may be found in the online version of this article.

*Correspondence to: Andreas Heyland, Integrative Biology, University of Guelph, ON, N1G-2L6, Canada. E-mail: aheyland@ufl.edu and Leonid L. Moroz, University of Florida, 9505 Ocean Shore Blvd, St. Augustine, FL 32080. E-mail: moroz@whitney.ufl.edu

Received 3 March 2010; Revised 8 September 2010; Accepted 12 October 2010

Published online 6 December 2010 in Wiley Online Library (wileyonlinelibrary.com). DOI: 10.1002/jez.b.21383

sequencing of several molluscan and annelid genomes and a growing number of large-scale transcriptome projects has recently been accomplished. These include the genome of the limpet *Lottia gigantea* (JGI), the snail *Biomphalaria glabrata* (Washington University, NCBI Project ID: 12879), the clam *Spisula solidissima* (Marine Biological Laboratory, NCBI Project ID: 12960), the planarian *Schmidtea mediterranea* (Robb et al., 2008), the leech *Helobdella robusta* (JGI), the polychate worm *Capitella teleta* (JGI), the transcriptomes of the mussel *Mytilus californianus* (JGI), the oyster *Crassostrea gigas* (JGI), the neuronal transcriptome of the sea hare *Aplysia californica* (Moroz et al., 2006) and the *Aplysia* genome project (Broad Institute, *A. californica* genome project). The availability of these resources represents a unique opportunity to perform comparative and genome-wide analyses of development on a transcriptional level.

The sea hare *A. californica* (Mollusca: Gastropoda: Opisthobranchia: Anaspidae) has been used extensively for physiological and cellular studies of behavior (Kandel, '79; Glanzman, '95; Leonard and Edstrom, 2004). Still, studies describing embryogenesis and larval development in this and related species are limited (but see Kriegstein et al., '74; Kriegstein, '77; Kandel, '79; Kandel et al., '80; Capo et al., 2009). Here, we analyze temporal and spatial gene expression changes during embryogenesis, larval development, and metamorphic stages using microarrays and in situ hybridization (ISH). Specifically, we monitor more than 39,000 unique transcripts from the recently sequenced *A. californica* neuronal transcriptome (Moroz et al., 2006) during development. By correlating relative gene expression levels with life history transitions, changes in body plan during development, as well as changes on the level of the larval, juvenile and adult nervous system, we provide novel insights into the development and neurogenesis of *Aplysia*. Specifically, we analyze transcriptional changes related to biomineralization and metamorphic stages as well as neurotransmitter and hormonal signaling mechanisms, and identify novel genes associated with these processes. Furthermore, we validate developmental changes in expression of selected transcripts using fluorescent and nonfluorescent ISH and RT-PCR. This is the first time that such an analysis was performed at the present scale in any lophotrochozoan species (but see Williams et al., 2009; Fiedler et al., 2010). This study, therefore, provides the foundation for future research on mechanisms underlying development, neurogenesis, and metamorphosis in *Aplysia* and other molluscs.

MATERIAL AND METHODS

Microarray

Microarray Design. Two custom 44,000 oligonucleotide arrays were constructed in collaboration with Agilent (Santa Clara, CA) Technologies using 60 mer oligonucleotide sequences designed

from each nonredundant sequence in the *Aplysia* EST database. We refer to the two arrays as: *Aplysia* Annotated Array (AAA) (GEO platform accession GPL3635) and *Aplysia* Discovery Array (DAA) (GEO platform accession GPL3636). All array files have been deposited on GEO (project accession: GSE14941). Additional details about the protocols used, including a list of features on each array, can be found on the GEO web site and are described in Moroz et al. (2006). We assembled all original contigs into 39,352 unique contigs. These contigs were used for all analyses presented in this article. A complete list of these contigs, annotation, and expression values can be found in Appendix 2.

Experimental Designs. We extracted RNA from eight developmental samples (Fig. 1), using an RNAaquous™ micro kit (Ambion, Austin, TX). mRNA was quantified using a Nanodrop ND1000 (Thermo Scientific), and quality was assessed using a Bioanalyzer™ 2100 (Agilent). We then added equal amounts of mRNA from each sample to a pooled sample, which was used for each hybridization. Appendix 7 summarizes details on biological samples used in the experiment as well as the names of original files submitted to GEO. All hybridizations were performed by Mogene Lc (St. Louis, MO).

Data Analysis. Methodologies for assessment of dye bias and normalization of this array are described in Moroz et al. (2006). Microarray files were filtered using ControlType (0). We then assembled all contigs from AAA and ADA into one master file and averaged expression levels of 60 mers belonging to the same nonredundant contigs (see above). Because we were primarily interested in gene expression profiling through all developmental stages, we did not perform any additional filtering at this stage.

Cluster Analysis. We performed k-cluster and hierarchical cluster analysis for the entire dataset (Appendix 3) and various subsets using SPSS v. 16. Parameters for hierarchical cluster analysis on the entire dataset were set using average linkages between groups with Pearson correlation. In addition to the final dendrogram, we also plotted the proximity matrix. K-means clustering was performed using 999 iterations and a convergence criterion of 0.02. The same criteria were used for k-cluster analyses on peptides and biomineralization-related genes.

GO Annotation and Enrichment Analysis. We were able to annotate 25% of all contigs (i.e. 9,879) using BLAST (NCBI and Swissprot), and from this dataset 3% (i.e. 1,108) could be annotated using automated GO annotation algorithms implemented in Blast2Go [36]. We then tested enrichment of specific GO categories within all the three developmental categories for all 1,108 contigs. All raw data from the analysis can be found in Appendix 4.

We used Fisher's exact test to compare GO categories for embryogenesis, larval development, and metamorphosis as adopted from (Bluthgen et al., 2005) and implemented in Blast2Go. To compare representation of specific GO groups between these three developmental categories, we compared GO graphs scores (exported

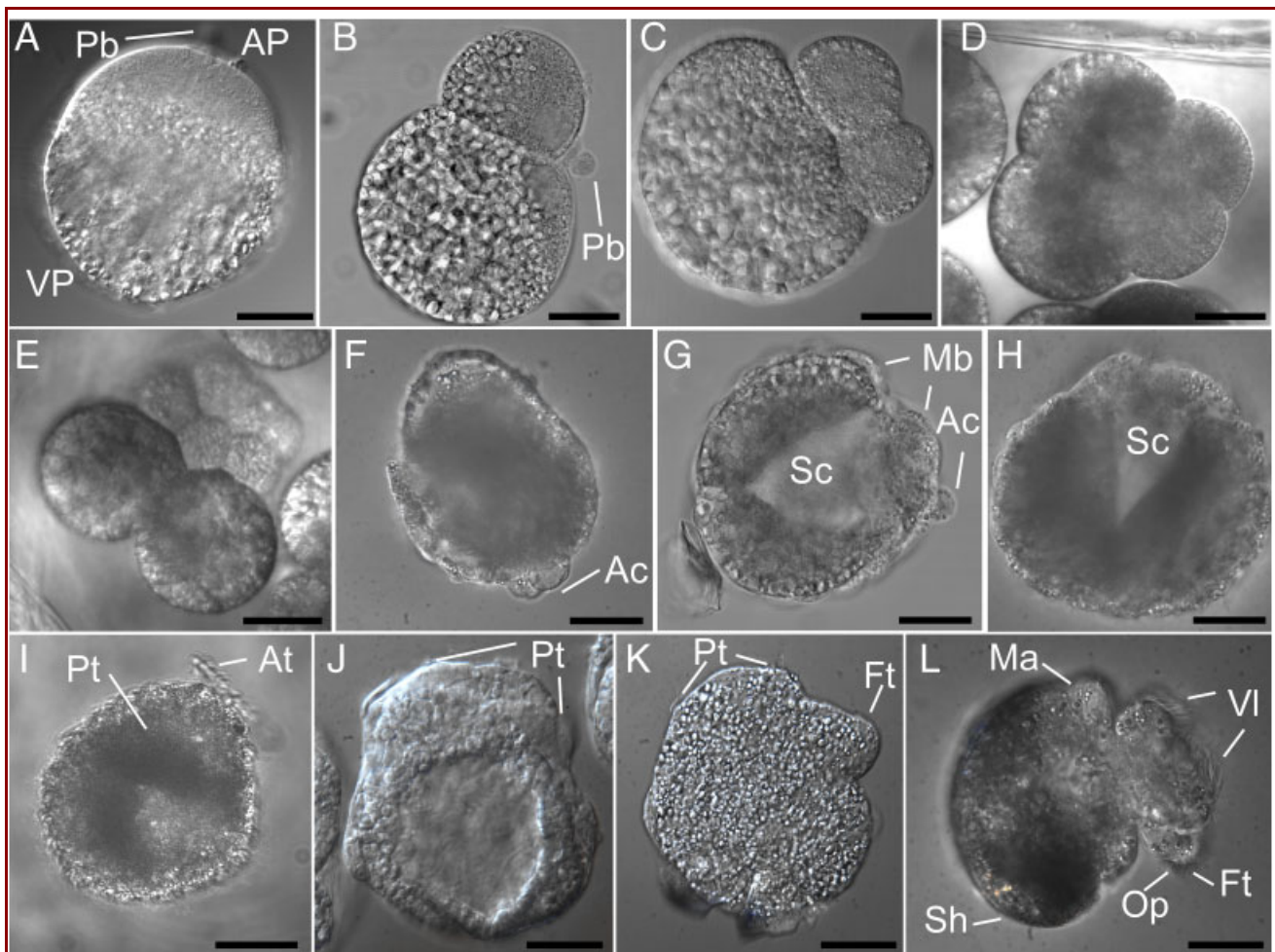


Figure 1. Prehatching development of *A. californica*. *A. californica* develops through unequal spiral cleavage inside a protective egg mass (A–E). The vegetal pole (VP) contains more yolk than the animal pole (AP), as can be seen in panel A. Polar bodies (Pb) are visible until approximately the third cleavage (C). Cells in the animal pole divide much faster than cells in the vegetal pole (C–E). Gastrulation occurs through epiboly (F–H). The segmentation cavity (Sc) is surrounded by the two macromeres (visible in panel C). In panel G, the mesotoblast cells (Mb) and anal cells (Ac) are both visible. After gastrulation (F–H), a trochophore larva (I) is formed inside this egg mass. The trochophore stage has a ciliated prototroch (Pt) and apical tuft (At). Note that the telotroch is missing in the image. Subsequently, early rudiments of the veliger body plan (J–L) become visible, such as the foot (Ft) and the velar lobes (VI). Before hatching from the egg mass, a complete veliger larva is formed (L). Scale bar sizes: A: 20 μ m; B: 21 μ m; C: 18 μ m; D: 20 μ m; E: 20 μ m; F: 35 μ m; G: 25 μ m; H: 22 μ m; I: 41 μ m; J: 32 μ m; K: 26 μ m; L: 35 μ m. Legend: Ac, anal cells; AP, animal pole; At, apical tuft; Ft, foot; Ma, mantle region; Mb, mesotoblast cells; Op, operculum; Pb, polar bodies; Pt, prototroch; Sc, segmentation cavity; VI, velar lobe; VP, vegetal pole.

from GO enrichment graphs in Blast2GO) and plotted the top five categories for each developmental category comparison (i.e. Embryo vs. Larva and Larva vs. metamorphosis). Although this method is not quantitative *per se*, it reflects the results of the enrichment analysis (see Appendix 4) and gives a qualitative picture of changes in gene expression organized by functional groups.

Reproducibility and Validation of Microarray Data. The microarray platform used in this experiment was extensively tested in

previous experiments, and details on technical reproducibility can be found in Moroz et al. (2006). The current microarray experiment was not repeated with biological replicates owing to financial limitations. Therefore, some caution should be used when using the absolute gene expression levels from this study. We did, however, take several important steps that should make the conclusions presented here more robust.

First, we only compare and discuss expression profiles of selected genes. Therefore, our conclusions are based on gene

expression trends as development progresses rather than absolute quantitative changes in expression. As we analyzed eight developmental stages, the probability of picking up “real trends” in expression levels is, therefore, enhanced.

Second, we selected seven genes from the dataset and tested their expression levels for all eight developmental stages using RT-PCR. These genes represent all major categories of expression profiles from the array, i.e. high expression early in development (cleavage and gastrula), during larval stages, and metamorphosis. They also represent different types of transcripts analyzed and further discussed in this study, i.e. peptides, RNA binding proteins, morphogens, and biomineralization genes. Finally, they contain genes that are expressed at both high and low absolute levels during development. Gastrulation was used as a baseline for expression levels. Specifically, we extracted RNA from eight developmental samples (Fig. 2F) using an RNAaqueous™ micro kit (Ambion). mRNA was quantified using a Nanodrop ND1000 (Thermo Scientific) and quality was assessed using a Bioanalyzer™ 2100 (Agilent). We used the kit's DNase treatment protocol to eliminate potential contamination with genomic DNA. cDNA synthesis was performed using the Superscript III First-Strand Synthesis System for RT-PCR (Invitrogen), following the manufacturer's recommendations. Random hexamers were used as primers. Quantitative real-time PCR (RT-PCR) reactions were prepared using the SYBR Green PCR Master Mix (Applied Biosystems), following the manufacturer's recommendations. Reactions were prepared in triplicate and run in an ABI PRISM® 7000 Sequence Detection System (Applied Biosystems). Relative abundance levels were calculated by the $\Delta\Delta C_T$ method (Applied Biosystems, 2004), using the ribosomal protein S5 transcript as an endogenous control (DA21976). All primer sequences used for RT-PCR are listed in Appendix 6. Relative abundance levels for RT-PCR data were calculated relative to the gastrula stage using the $\Delta\Delta C_T$ method (Applied Biosystems, 2004). Microarray data for selected transcripts were converted to the same format by using the difference between the developmental stage and gastrula as the power of ten (conversion to fold change). All relative expression levels of the gastrula stage are, therefore, one and were removed from the dataset for the correlation analysis. We then tested the correlation using two-tailed Pearson correlation analysis of these 48 datapoints. We used RT-PCR to validate seven contigs from the microarray for all eight developmental stages. Correlation analysis using Pearson's correlation coefficients r^2 is 0.93.

Third, we tested gene expression profiles using ISHs of selected transcripts. Although this is not an inherently quantitative method to validate gene expression levels, it provides a qualitative assessment of gene expression profiles during development. In general, we found good correlations between our microarray experiments and ISH patterns.

Finally, we compared the expression profile of specific genes known from other experiments to our microarray study and found that our array data generally reflect a high degree of reproducibility for those genes. Examples are discussed throughout the text.

We feel that these four precautions add a significant amount of validity to our dataset. Still, biological replicates were not performed, and consequently the statements about expression levels should be viewed as hypotheses that can be tested in future experiments using RT-PCR or ISH.

Gene Annotation. We performed gene annotation of all 39,352 unique contigs using Blast2GO (Gotz et al., 2008). In the first step, all contigs were blasted (*blastx*) against Swissprot and nr databases as implemented in Blast2GO using an E-value of 10^{-3} . The top five hits were stored from this analysis. In the next step, blast results were mapped and then annotated using Blast2GO default parameters (hit filter: 10^{-6} ; presimilarity hit filter 30; annotation cutoff: 55; GO weight: 5). GO annotations for the entire dataset can be found in Appendix 2. Note that biomineralization genes and secretory products and peptides were annotated manually.

Annotation of biomineralization-related genes. We carried out a thorough literature screen that resulted in a list of 522 genes, including known biomineralization genes (Jackson et al., 2006), bioinformatically identified biomineralization genes in the genome of the sea urchin *Strongylocentrotus purpuratus* (Livingston et al., 2006), and genes that were identified in a recent secretome assay in *H. asinina* (Jackson et al., 2006). Sequences for the genes of interest were obtained from the Sea Urchin Genome Project webpage at BCM (<http://annotation.hgsc.bcm.tmc.edu/Urchin/cgi-bin/pubLogin.cgi>), NCBI's RefSeq (<http://www.ncbi.nlm.nih.gov/RefSeq/index.html>), and NCBI's GenBank (<http://www.ncbi.nlm.nih.gov/Genbank/>). Sequences were split into those annotated as proteins and those as genes. Protein sequences were blasted (tBLASTn 2.2.10, E-value ≤ 0.1 , Matrix: Blosum62) against the *Aplysia* EST database (Moroz et al., 2006), likewise nucleotide sequences were blasted directly against the EST-database (BLASTn 2.2.10, E-value ≤ 0.1 , Matrix: Blosum62) in a local BLAST. BLAST result files were parsed with PLAN (He et al., 2007) to extract best hit tables for the query sequences. Owing to the nature of the approach (e.g. many biomineralization genes belong to gene families), numerous query sequences returned the same ESTs as the best hit in *Aplysia*. For this reason, the *Aplysia* EST identifier was used to query the *Aplysia* expression database. To substantiate annotation of *Aplysia* ESTs, sequences were additionally searched with *blastx* against NCBI nr database with a cutoff E-value of $1e^{-3}$.

Annotation of Peptides and Secretory Products. We used custom BioPerl scripts to find all open reading frames (ORF) of the 39,352 contigs. These ORFs were then screened for peptide cleavage sites and signal peptide predictions using SignalP 3.0 (Nielsen et al., '97). A complete list of these putative peptides and secretory products can be found in Appendix 2.

In Situ Hybridizations. We performed two types of ISHs: (1) WMISH using the Elmer Perkin TSA-FITC (NEL741) and (2) nonfluorescent ISH utilizing digoxigenin (DIG)-labeled

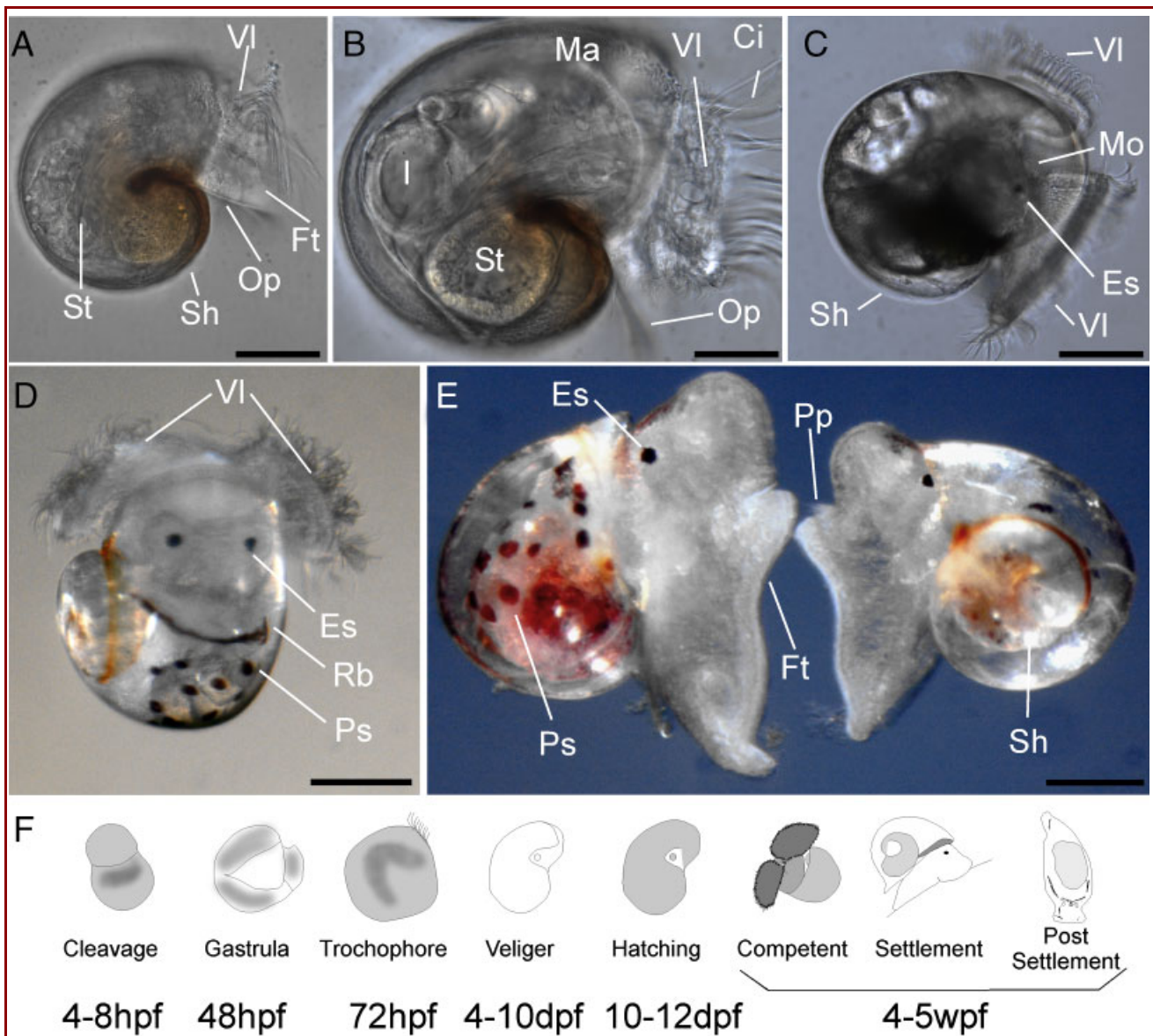


Figure 2. Posthatching development and metamorphosis of *A. californica*. After hatching, the veliger larva will develop over an extended period of time (up to 3 weeks) in the plankton until all adult organs and the complete adult nervous system are formed (A–E; see Fig. 3). Only small changes in external morphology are visible during this time, but major changes occur internally, such as the development of the nervous system (see Fig. 3), the heart, and the excretory system. At the end of the planktonic period, the *Aplysia* veliger larva will reach metamorphic competence (D). Morphological characters for this stage are the occurrence of pigmented spots (Fig. 2D; Ps) and a red band that is visible on the mantle margin (Rb). Within 12–24 hr, competent larvae will transform into a settled juvenile (E; see Fig. 3). We are using the symbols indicated in panel F to describe the following stages: (I) early cleavage, (II) gastrulation, (III) trochophore, (IV) first veliger, (V) hatching, (VI) metamorphic competence (stage 6; see text for details), (VII) postmetamorphosis (stage 7; see text for details), and (VIII) 60 hr postmetamorphosis. The numbers below the icons indicate the approximate time line of embryonic and larvae development, based on our own observations at 20°C. Ci, cilia; Es, eyespot; I, intestine; Ma, mantle region; Mo, mouth; Op, operculum; Pp, propodium; Ps, pigment spot; Sh, shell; VI, velar lobe; St, stomach. Panel E modified from (Heyland and Moroz, 2006). Scale bars: A: 45 μ m; B: 50 μ m; C: 90 μ m; D: 90 μ m; and E: 90 μ m.

antisense RNA probes with nitro blue tetrazolium chloride/5-bromo-4-chloro-3-indolyl phosphate (NBT/BCIP) as the alkaline phosphatase substrate for detection of single mRNA species. ISH probes were synthesized according to the manufacturer's directions (13 μ L template, 2 μ L NTP labeling mix, 2 μ L $10 \times$ transcription buffer, 1 μ L RNase inhibitor, 2 μ L SP6 or T7 RNA polymerase, 37°C for 2 hr) with the following modifications. We used 7 μ L of template (cleaned and cut plasmid prep) with 1 μ L of $10 \times$ RNA polymerase buffer, 1 μ L of DIG (DIG RNA Labeling Kit (SP6/T7), Roche; Cat. No. 1175025), 1 μ L Sp6/T7/T3 RNA polymerase, and 1 μ L of RNasin (or any RNase inhibitor is fine) and incubated for 3.5 hr at 37°C. We then added 1 μ L of DNase1 (NEB M0303S) and incubated for 15 min at 37°C. After digestion, we added 1.5 μ L of 7.5M LiCl₂ and 50 mM EDTA solution plus 38 μ L of 100% Ethanol (EtOH), mixed gently and kept at -20°C overnight for precipitating the RNA. The next morning, we spun the reaction for 20 min at 15,000 rpm at 4°C and removed the supernatant without disturbing the pellet. We rinsed RNA with 70% EtOH and spun again for 5 min at 4°C at 15,000 rpm. After letting the pellet air dry for 5 min, we redissolved it in distilled water (DW-20 μ L) and ran 1 μ L on a 1% gel to test the integrity of the RNA probe.

In Situ Hybridization. We fixed embryonic stages in a MOPS buffer-based fixative (0.1 M MOPS; Sigma, St. Louis, MO, M5162 at pH 7, 0.5 M NaCl, 4% paraformaldehyde, Diethyl pyrocarbonate (DEPC) treated water) for 3–5 hr at 4°C. Next, we dissected embryos from the egg mass in MOPS buffer (0.1 M MOPS at pH 7, 0.5 M NaCl, DEPC-treated water), washed them five times for 10 min each and dehydrated through two changes of 70% EtOH in DEPC-treated water and stored them in 70% EtOH at -20°C until further processing. Larval and juvenile stages were anesthetized at room temperature (RT) in isotonic MgCl₂ solution (337 mM; in distilled water) for 10 min and then transferred on ice for another 10 min. We then fixed larvae and embryos overnight at 4°C in MOPS buffer-based fixative and washed samples five times in MOPS buffer for 10 min each. To remove the shell, we transferred larvae into 0.5% trypsin (Type 1 from bovine pancreas; Sigma: T8003) for 15 min, washed larvae three times in MOPS buffer, and exposed them to 10% EDTA in MOPS buffer for 45 min at RT and pH 7. Finally, we rinsed samples three times in MOPS buffer, dehydrated three times in 70% EtOH, and stored samples in 70% EtOH at -20°C until further processing.

Samples were rehydrated in MOPS buffer (three washes for 10 min each) and treated for 10–30 min (depending on developmental stage and batch of eggs) with proteinase K (0.58 μ L/mL; Roche Diagnostics). We stopped the reaction with 0.2% glycine in MOPS buffer (two changes) and washed samples two times in MOPS buffer before postfixing them in 4% paraformaldehyde in MOPS buffer for 30 min. We washed samples three more times in MOPS buffer (10 min each) and subsequently exposed them for

30 min to 3% peroxide solution in MOPS buffer at RT, to quench endogenous peroxidase and alkaline phosphatase activity. After another three washes in MOPS buffer, we proceeded to the hybridization steps.

We prehybridized samples two times in hybridization buffer at RT for 20 min each (50% formamide, 0.1 M MOPS at pH 7, 0.5 M NaCl, 0.1% Tween-20, 1 mg/mL Bovine Serum Albumin (BSA; in milli-Q water)) and distributed small subsamples (30–100 embryos/larvae) into the wells of a 96-well plate with round well (Costar RK-01959-28). We then performed the second prehybridization step at the temperature required for the probe for 1–3 hr. We premixed probes in 100 μ L hybridization buffer, denatured them at 95°C for 10 min, and kept them on ice until further use (not more than 20 min). After complete hybridization, we added the premixed probe to the samples and incubated overnight at the protocol specific temperature.

We performed all further steps using a p300 12-channel pipette, removing approximately 200 μ L of solution from wells and replacing them with new solution. Note that the samples were not removed from the original well after this stage. First, we washed samples five times with MOPS buffer (10 min each) at hybridization temperature. We then added three further washes with MOPS buffer at RT (10 min each). Next, we exposed samples to block solution 1 (0.1 M MOPS at pH 7; 0.5 M NaCl; 10 mg/mL BSA; 0.1% Tween-20; milli-Q water; 10% goat serum) for 20 min at RT, block solution 2 (0.1 M MOPS at pH 7; 0.5 M NaCl; 10 mg/mL BSA; 10% goat serum; 0.1% Tween-20; milli-Q water; 10% goat serum) for 30 min at 37°C, added anti-DIG antibody in block solution to the wells (0.1 M MOPS at pH 7; 0.5 M NaCl; 10 mg/mL BSA; 10% goat serum; 0.1% Tween-20; milli-Q water; anti-DIG antibody at 0.75 U/ μ L; Roche Diagnostics) and incubated at RT overnight.

The next day, we washed samples six times in MOPS buffer (1 hr each) at RT, added alkaline phosphatase buffer (0.1 Tris at pH 9.5; 50 mM MgCl₂; 0.1 M NaCl; 1 mM levamisole; milli-Q water) to the wells and incubated twice for 30 min. Finally, we added staining solution (10% dimethyl-formamide; 0.1 Tris at pH 9.5; 50 mM MgCl₂; 0.1 M NaCl; 1 mM levamisole; milli-Q water; 75 mg/mL NBT/BCIP; Roche Diagnostics) to the samples. Once the signal was sufficiently strong, we stopped the reaction with MOPS buffer and dehydrated samples in 70% EtOH and stored them at -20°C until further use. For imaging, we transferred samples into 100% glycerol.

Whole Mount Fluorescent In Situ Hybridizations. For MWISH, we used the same protocol as for ISH with several important differences. The probes were detected using Anti-Digoxigenin-POD, Fab fragments antibody (Roche: 11207733910). Revelation was carried out using the Elmer Perkin, TSA amplification system (NEL741) following manufacturer's instructions. Note that fluorescence intensity in embryos and larvae was checked every 15 min during development and compared with controls.

Embryonic and Larval Cultures and Animal Preparation

A. californica adults were collected by Santa Barbara Marine Biologicals and were housed in the flow-through seawater system at the Rosenstiel School of Marine and Atmospheric Science or at the Whitney Laboratory for Marine Biosciences as described by Capo et al. (2009). Egg masses from *Aplysia* were collected early in the morning. We then separated individual egg ribbons from each other and rinsed them carefully with filtered seawater. Ten to twenty individual pieces off egg ribbon (5–10 cm) were then placed into glass dishes with filtered (0.2 μm) seawater and kept at RT until hatching. Water was changed every day by transferring all egg ribbons into a new dish.

We sampled embryos and larvae according to the staging scheme represented in Figures 1 and 2. For cleavage stages, we collected embryos between the two and eight cell stage, and for gastrula we collected embryos that were anywhere between the onset of gastrulation (Kandel, '79) (Fig. 1G) and the final stages of epiboly (Fig. 1H). Trochophore stages were identified by the presence of the apical tuft as depicted in Figure 1I. Veliger stages were collected once the velar lobes, the shell, and the foot were visible (Fig. 1L). Hatching stages were collected immediately after hatching occurred (within 1–2 hr). Metamorphically competent larvae were collected when pigment spots were visible and more than 50% of a subset of larvae from a given population had settled. Settled larvae were collected immediately after settlement on algae. The same population was subsampled 60 hr after settlement.

For WMISH, egg strands were cut into 1 cm long pieces and placed into purified seawater (0.22 μm) containing 3.5% MgCl_2 . Strands were incubated overnight at 4°C in an in situ fixative (ISF) containing ultrapure 4% paraformaldehyde (Electron Microscopy Sciences, Hatfield, PA: 15710) in 0.1 M MOPS (Sigma: M1254), 2 mM MgSO_4 (Sigma: M2643), 1 mM EGTA, and 0.5 M NaCl (Sigma: S3014). After rinsing strands several times in Phosphate Buffered Saline (PBS), embryos and larvae in egg cases were removed using fine forceps and scissors. Fixed samples were then rinsed twice with PBS, washed three times with 100% EtOH, and stored at –20°C in 70% ethanol until further use. Posthatching larval stages were fixed following procedures previously described (Marois and Carew, '97a). Larvae in seawater were placed for 20 min on ice in 3.5% MgCl_2 and then fixed in ISF overnight. After fixation, larvae were washed three times with 100% EtOH and stored at –20°C in 70% ethanol until further use.

RESULTS AND DISCUSSION

Earlier reports dealing with opisthobranch development, from the late 1800s (Blochmann, '83), provide a basis for comparing the development of *Aplysia* with related sea hares (Kandel, '79). Specific data for *A. californica* primarily focus on later larval stages. For example, Kriegstein ('77) and others (i.e. Capo et al., 2009) provided a detailed description of *A. californica* posthatching development. Several more recent descriptions

dealt with *A. californica* metamorphosis (Heyland and Moroz, 2006) or the development of specific structures, such as the nervous system (Dickinson and Croll, 2001; Wollesen et al., 2007) and muscles (Wollesen et al., 2008). Because there is currently no complete photographic documentation of *A. californica* embryogenesis and larval development available (but see <http://Aplysia.miami.edu/>), we summarize available literature in the context of our own photographs of *Aplysia* development presented in Figures 1 and 2. We then characterize transcriptional changes as a function of these developmental stages, focusing on biomineralization, metamorphosis, and endocrine and neuroendocrine signal transduction mechanisms. Finally, we compare the developmental transcriptome of *Aplysia* with similar studies in one other mollusc species, *D. melanogaster*, *C. elegans*, and the zebrafish *Danio rerio*, to gain a first insight into interesting similarities and differences between these species.

Description of *Aplysia californica* Development

Embryonic and Larval Stages. The earliest stages of *A. californica* development occur within an encapsulated egg mass that is laid by these hermaphroditic animals within a few hours after mating. Each egg mass consists of egg capsules and each capsule contains 5–10 embryos, which develop through unequal spiral cleavage. In Figure 1, we summarize the prehatching period of the *Aplysia* life cycle and show representative images of the main phases. The photos and description are based on previously published work (Kandel, '79; Capo et al., 2009) and our own observations. The first cleavage (Fig. 1A and B) occurs 4–7 hr after egg masses are laid. Early spiral cleavage patterns of *A. californica* as well as gastrulation (see Fig. 1A–G) are similar to the Atlantic species *Aplysia punctata* (Kandel, '79). Gastrulation occurs after the seventh to eighth division and involves epiboly, a process by which micromeres from the animal pole of the embryo begin migrating over the surface of the embryo. Cellular and molecular mechanisms underlying this process have never been investigated.

After 2–3 days, the trochophore larva (Fig. 1I) is forming. In *A. californica*, the trochophore stage is formed inside the egg mass. This is in contrast to several other lophotrochozoan clades where the trochophore larva is free living. Therefore, the morphology of the *Aplysia* trochophore is simplified in comparison to free living trochophore stages, although the apical tuft, prototroch, and telotroch are all present (see Fig. 1I). The transition from trochophore to veliger body plan occurs on days 3–4 of development (Fig. 1J and K). In the first veliger stage, the first rudiments of the shell become visible and the trochophore prototroch transforms into the velar lobes (Fig. 1K and L). During this time, the larva undergoes torsion as well as flexion, prominent events in gastropod embryogenesis that consist of the rotation of the anus and visceral mass in relation to the head and foot (Page, 2003).

The prehatching veliger larva has a completely formed shell, larval stomach, velar lobe, kidney, heart, mouth, and muscles, and it is swimming actively within the egg mass. These veliger larvae can retract into the shell when disturbed. After 7–10 days postfertilization, the veliger larva will break out of the egg mass and begin swimming in the plankton. During this life history transition, the larva begins feeding on phytoplankton by means of the velar lobes (Fig. 1L). In addition, velar lobes are used for swimming (see Fig. 2 and Appendix 1).

Posthatching larval development in sea hares has been traditionally divided into six distinct stages (Kriegstein et al., '74; Kriegstein, '77), some of which are illustrated in Figure 2. The planktonic phase lasts approximately 4–5 weeks and involves the formation of various novel structures, whereas some existing structures will be eliminated or transformed. New structures include the eyes, the complete adult ganglionic nervous system, adult heart, muscular foot, and various epithelial components, including distinct pigmentation patterns in the skin (Fig. 2A–D). Toward the end of the planktonic period, the veliger larva will attain metamorphic competence (Fig. 2D), a stage during which it becomes sensitive to specific environmental cues which can induce settlement and subsequently metamorphosis (Kriegstein et al., '74; Kriegstein, '77; Chia and Rice, '78; Capo et al., 2009). The exact chemical identity of these cues is still unknown for *Aplysia*.

The most notable morphological changes during metamorphosis as well as changes on the level of the nervous system are illustrated in Figure 3. Based on several previous descriptions (Kriegstein et al., '74; Kriegstein, '77) and our own observations, behavioral changes during the metamorphic transition can be categorized as either locomotory or related to feeding (Fig. 3A). Note the distinction between metamorphosis and settlement: in *Aplysia*, settlement behavior is reversible, in that the veliger larva can temporarily be attached to the substrate and then released from it again. Once it has found a suitable settlement site, it initiates metamorphosis by releasing its velar lobes. Therefore, metamorphosis is irreversible.

A number of studies also describe postsettlement development of *Aplysia* (Kriegstein et al., '74; Kriegstein, '77; Kandel, '79). After settlement, the juvenile snail will undergo further morphological changes before it eventually transforms into a fully formed small sea slug (Fig. 2E and F) that contains the majority of adult structures. Major changes during the juvenile and adult phase include the internalization and reduction of the shell (the shell is not visible in mature animals) as well as the development of the reproductive system.

In the present microarray experiments, we used eight developmental stages (early cleavage, Cl; gastrulation, Ga; trochophore, Tr; early veliger, Vel; hatching, Ha; metamorphic competence, PreM; postsettlement, PostM; and 60 hr postsettlement, Juv) that are schematically illustrated in Figure 2F. These stages provide a coarse representation of *Aplysia* development

(note that the approximate developmental times postfertilization at 20°C are shown in Fig. 2F). They also frame some of the major morphological, physiological, and ecological transitions in the *Aplysia* life cycle, i.e. hatching and metamorphosis. Note that we only sampled three stages during the metamorphic transition in this experiment (competence, settled larva, and postsettled juvenile; see Materials and Methods for more details). Expression patterns during the transition are, therefore, specific to these stages and not representative for the metamorphic transition *per se*. We used a discrete scale on the x-axis of all figures to summarize temporal expression patterns. We made this choice for practical reasons, as the larval development of *Aplysia* is close to 4 weeks, whereas time differences between embryonic stages are only a few hours.

Embryonic and Larval Nervous System. The nervous system of *A. californica* larvae consists of two components: the apical sensory organ (ASO; Fig. 3B–D) and a juvenile ganglionic nervous system (Fig. 3E). The ASO fulfills important functions in processing environmental information throughout development (Page, 2002; Kempf and Page, 2005; Heyland and Moroz, 2006). It is located in the posterior region to the eye spots and begins forming during the trochophore–veliger transition (Marois and Carew, '97a,b,c; Dickinson et al., 2000; Dickinson and Croll, 2001). In many mollusc species, the ASO contains several serotonin-(5-HT) containing cells, and 5-HT acts both as a regulator of prototrochal ciliary activity in encapsulated and free living stages (Page, 2002) as well as a modulator of sensory input to the ASO (Diefenbach et al., '91; Couper and Leise, '96; Marois and Carew, '97a; Page, 2002). Therefore, the ASO likely has both sensory and motor function, as previously pointed out (Mackie et al., '76; Marois and Carew, '97a).

Adult ganglia can be detected as early as the veliger stage and they likely appear during the trochophore–veliger transition (Kriegstein, '77; Kandel et al., '80; Dickinson et al., 2000). We summarize the developmental phases of the *Aplysia* ganglionic nervous system in Figure 3E (based on personal observations and previous description by Kriegstein, '77; Kandel et al., '80). Posthatching veliger larvae contain cerebral and pedal ganglia as well as eye stalks. Posterior ganglionic components of the visceral loop are added during later larval development. As a result, the metamorphically competent larvae contain all ten adult type ganglia (Fig. 3E). Critical adult behaviors, such as feeding and crawling, are established immediately before or during the metamorphic transition.

As first summarized by Kandel et al. ('80), adult feeding behavior consists of an appetitive and a consummatory response to food. In the appetitive response, the animal is rearing up its head and waves it from side-to-side. In the consummatory response, the juvenile displays a so called “all-or-none” ingestive movement of the buccal mass and radula (Kandel, '79; Kandel et al., '80). Both behaviors emerge after settlement of Stage 6

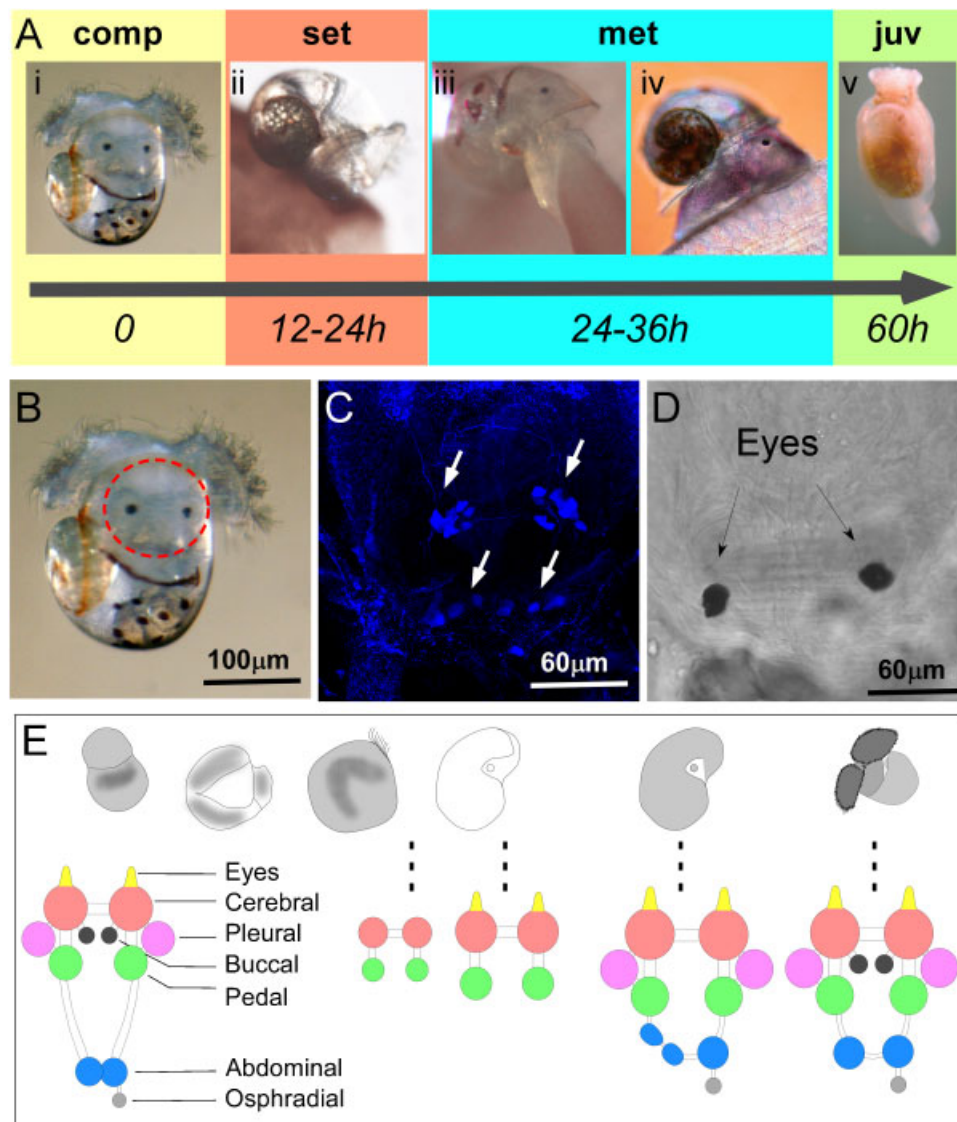


Figure 3. (A) Time course of metamorphic transition and neurogenesis in *A. californica*. *A. californica* transforms from a competent swimming veliger larva (*comp*; stage 6; Fig. 2D) into a grazing juvenile sea hare in approximately 60 hr (Fig. 2E). The first sign of metamorphosis (*met*) is the shedding of the velar lobe. Before metamorphosis, the larva explores the future settlement substrate for 12–24 hr under standard laboratory conditions (20°C in a glass dish). In contrast to metamorphosis, settlement behavior is reversible. Upon shedding the velar lobe, the two major changes in locomotion and feeding behavior are taking place. The larva transitions from swimming to crawling behavior and begins feeding on algae using buccal mass movements. Further morphological changes involve internalizing of the shell and reducing its size. These result in a juvenile *Aplysia* (*juv*), which largely resembles the adult sea hare (approximate size 3 mm). Behavioral changes during the metamorphic transition involve rewiring of neuronal connections and the destruction of the larval nervous system (B–D). A competent *Aplysia* larva (B) has two distinct nervous systems: larval and adult. A small part of the larval neurons are serotonergic and can be visualized using 5HT (serotonin) antibody (C). Region circled in B is magnified in C and D. C and D are identical view of the larval nervous system, C indicated staining with 5HT antibody, and D indicates corresponding DIC image. Previous studies have shown that no larval neurons are transferred to the adult stage (Marois and Carew, '97a,b,c). Serotonergic neurons in the larval apical sensory organ (ASO) are indicated in C. The adult nervous system begins to form during late embryonic development, and cerebral and pedal ganglion can be identified as early as in the prehatching veliger stage (E).

(metamorphic competence) larvae, as can also be seen in the video (Appendix 1). In contrast to other reports (Kriegstein et al., '74; Kandel, '79; Kandel et al., '80), this adult feeding behavior including both components was not established until 24–36 hr postsettlement when the animal is beginning to ingest food (personal observation).

Identification of Stage-Specific Transcription Patterns During *A. californica* Development

To capture dynamic changes in transcription during development, we performed a series of cluster analyses with the stage-specific expression levels of all contigs (Fig. 4). The heatmap in Figure 4A shows relative gene expression levels translated into a color range from green (minimum value -2.0) to red (maximum value $+2.0$) based on all 39,352 unique contigs (contiguous sequences). The values represent the logarithm (base 10) of the fold change, consequently ranging from -100 to $+100$ relative to the reference sample, which consisted of equal amounts of RNA from each sample used in this experiment (see Materials and Methods for more details on experimental design). GenBank and Swissprot accession numbers (when applicable from our transcriptome annotation) for the complete dataset with IDs, annotation, and relative expression levels are reported in Appendix 2. In the text, we refer to the microarray accession numbers when discussing specific transcripts.

The dendrogram pattern above the heatmap reflects the relative similarity of the expression patterns among developmental stages, based on a hierarchical cluster analysis. Values of the proximity matrix can be found in Appendix 3. Based on this analysis, we distinguish between four major clusters of developmental stages: (i) cleavage; (ii) gastrulation; (iii) larval stages inside the egg mass (Cluster 2A; Fig. 4A); and (iv) metamorphic stages (Cluster 2B; Fig. 4A). We used these observations to form three nonexclusive categories and analyzed enrichment patterns of gene ontology (GO) categories (Gotz et al., 2008). Note that we had to regroup the clusters as only a small fraction of the genes used on the microarray could be annotated using gene ontologies. The categories we chose are, therefore, a compromise between the categorizations resulting from the cluster analysis, the availability of GO annotations, and distinctions between developmental stages that are biologically relevant. The following criteria were used for initial categorization. Phase 1, consisting of early cleavage stages and gastrulation (phase 1; Fig. 4A), are stages that are likely expressing primarily maternal transcripts. Phase 2 consists of all veliger stages (phase 2; Fig. 4A) and phase 3 are all metamorphic stages (phase 3; Fig. 4A). The list of all annotated sequences specific to each established cluster of development can be found in Appendices 2 and 4.

Little information exists on the onset of zygotic transcription in molluscs and we were unable to measure gene expression levels for unfertilized eggs in *A. californica* in this study. Based on the transcription profiles on the array, early cleavage and

gastrula stages are very distinct from later stages (phase 1 Fig. 4), such as trochophore and veliger stages. Based on available literature (i.e. Andeol, '94), it is likely that the majority of transcripts during these stages are maternally provided. This is based on an analysis of the midblastula transition in a leech in comparison to other animal species (Andeol, '94). Other, more direct comparisons of midblastula transitions in mollusks and specifically in *Aplysia* are not available. In addition to the hierarchical cluster analysis, we also generated k-means clusters of developmental gene expression (see Appendix 5). This analysis provides us with insights into groups of genes with distinct expression profiles, and therefore complements the hierarchical clustering analysis.

Gene Expression Specific to Embryonic Development. Among annotated transcripts, we detected enrichment of genes associated with chromatin remodeling, chromosome and nuclear functions, cell cycle, RNA processing, and transcriptional regulation during early embryogenesis (Fig. 4B and C). These functions are consistent with extensive cellular division and differentiation. For example, Ras-related nuclear proteins (DA1390) and Ran-binding proteins (DA10059) are essential for RNA and protein trafficking, as well as DNA synthesis and cell cycle progression (Ren et al., '93). In addition, we detected a diversity of transcripts coding for RNA binding proteins, such as Yantar (DA55121), which were expressed at elevated levels during cleavage stages.

An emphasis on RNA metabolism and trafficking also emerged from our data, after analyzing gene expression profiles during development (Appendix 5; Clusters 4 and 15). A significant number of transcripts expressed during cleavage are coding for RNA helicases, including members of the DEAD-box protein superfamily (Appendix 4), which are involved in a variety of metabolic processes involving RNA (Linder, 2000, 2006). DEAD-box polypeptide 47, from *Aplysia* (DA9989), was used to validate this microarray experiment with RT-PCR (see Appendix 6 for details and other transcripts used for the validation).

The majority of signal peptides and secretory products are expressed during later developmental stages (discussed below). Still, some transcripts with known function in the nervous system, such as Apolipoprotein D (apoD) (DA22583) and Ependymin (DA1895), have relatively high expression levels during embryogenesis. ApoD is a multiligand, multifunctional glycoprotein with putative functions in the nervous system (Rassart et al., 2000). Ependymin is a glycoprotein involved in a diversity of functions ranging from neuroplasticity to regeneration that was only recently identified in a number of invertebrate genomes (Suarez-Castillo and Garcia-Ararras, 2007). A specific role in development has not been proposed for either of these proteins. We also annotated several other transcripts with expression patterns comparable to ependymin and ApoD (Cluster 5, Appendix 2). Illustrative examples include escargot



(esc) and a pannexin, most similar to pannexin-3 (DA37538). *Esc* (DA22352) is a transcription factor that is critical for asymmetric cell division during *D. melanogaster* CNS development (Cai et al., 2001). Pannexins are a broad family of gap junction-forming proteins (Panchin, 2005) that were originally identified in *Aplysia* neurons (Moroz et al., 2006). Their expression, early in embryogenesis, is consistent with extensive intercellular communication processes following gastrulation and, possibly, early stages of neurogenesis.

Gene Expression Specific to Larval Development. The transition from embryo to veliger larva involves an intermediate trochophore stage. Early veliger larvae have specialized muscular, sensory and nervous systems, and begin to form internal organs. Putative transcriptional changes related to organogenesis are best reflected in genes from Cluster 1 (Appendix 2). They include transcripts associated with well known neuronal signaling peptides, such as myomodulin-like peptide (DA22071), cardioactive peptide (DA22239), a synthetic enzyme for serotonin (5-HT), and a G-protein-coupled 5-HT receptor (DA48185) (Fig. 5). Data on expression levels of essential 5-HT signaling components (i.e. receptors, synthesis enzymes, and transporters) further confirm that the serotonergic nervous system is active at the trochophore to veliger transition (Fig. 5). Fluorescent ISHs on some of these transcripts (Fig. 5) also suggest a considerable overlap of gene expression patterns with previously published expression patterns using 5-HT antibodies (Fig. 3C; Marois and Carew, '97a,b,c). Note that only a subset of cells expresses both, 5HT and TryMO. Further analysis will be required to characterize the cells expressing these genes.

The trochophore-veliger transition is also characterized by specific GO categories related to muscle development and signal transduction events. Examples from within these categories include syntrophins (DA11151), which have known functions in heart and skeletal muscle development. We also detected enrichment of transcripts related to vesicle transport and secretion (Fig. 4B–D). Proteins encoded by these transcripts could have various, yet unknown, functions related to hormonal or neuronal signaling. However, based on the GO annotation of these transcripts, we hypothesize that established interneuronal (synaptic) communication pathways may exist in larvae. This hypothesis can be addressed by analyzing the spatial expression patterns of these secreted products during *Aplysia* development using antibodies. Still, the highest level of expression of secretory products was observed in metamorphic stages, which we discuss below.

One secreted product that is expressed at elevated levels during the trochophore veliger transition is secreted frizzled-related protein 2 (DA36868). Members of this transmembrane protein family function as Wnt receptors. Secreted frizzled-related proteins can act as modulators of Wnt signaling along with a suite of other activators and repressors, some of which

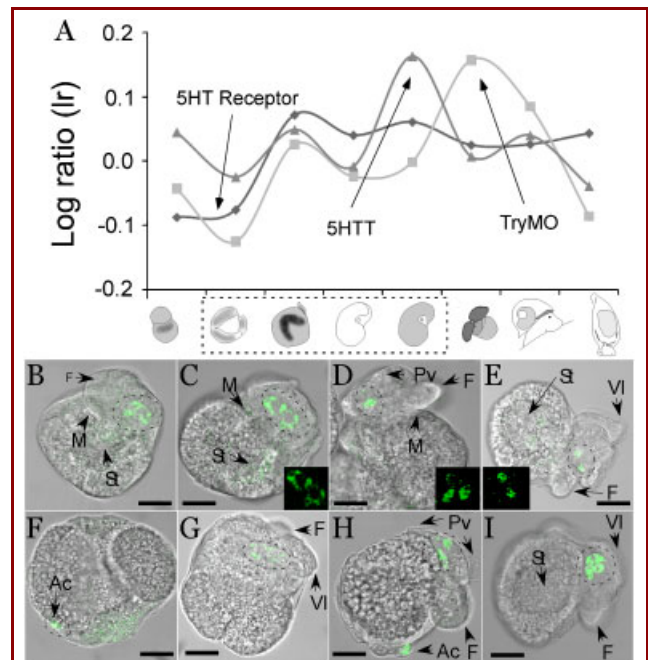


Figure 5. Serotonin (5-hydroxytryptamine; 5HT) transporter (5HTT) and 5HT synthesis enzyme (TryMO) are expressed in serotonergic neurons of the adult ganglionic nervous system inside the larva as early as pre-hatching. 5HT is an important signaling molecule in the larval nervous system, as several studies from molluscs and other animals with larval development have shown (see Fig. 3). We identified 5HTT, TryMO, and 5HT receptor sequences in the *Aplysia* transcriptome and analyzed their relative expression patterns during development (A). We then analyzed the expression patterns qualitatively using MWISH in trochophore and pre-hatching veliger stages. Note that the stages used for in situ hybridizations are indicated in panel A by a dashed box. 5HTT (B–E) and TryMO (F–I) both localize in cells of the adult nervous system of early and late veliger stages (green staining). These cells have been previously shown to be serotonergic (Marois and Carew, '97b). Stages are as follows: B/F Trochophore–Veliger transition (Fig. 1J); C/G early veliger stage (Fig. 1K); D/H later veliger stage; and E/I veliger stage at hatching (Fig. 1L). Inserts are three dimensional reconstructions from confocal microscope stacks of serotonergic cells shows in the DIC-FITC merge. Negative controls (sense) probe were performed and did not result in any specific staining pattern, with the exception of the ubiquitous background stain in the stomach region. (data not shown). Also note that only a subset of cells express both TryMO and 5HTT. Ac, anal cells; F, foot; M, mouth; Pv, prevelum; St, stomach; VI, velar lobe. Scale bars: B: 42 μ m; C: 45 μ m; D: 50 μ m; E: 80 μ m; F: 40 μ m; G: 45 μ m; H: 50 μ m; I: 75 μ m.

remain to be characterized in detail (Melkonyan et al., '97). The fact that frizzled-related protein is expressed at elevated levels during the trochophore to veliger transition is an interesting

finding, but future studies will have to address the role of Wnt signaling in this transition, and specifically the function it may have in nervous system patterning of the veliger larva.

Transcription Levels Characterizing Metamorphic Stages. The separation of metamorphic stages from other larval stages in both the hierarchical and k-means cluster analysis (Fig. 4; Appendices 2 and 5) indicates that a fundamentally different developmental program is turned on during metamorphosis. Note that significant changes in gene transcription were also detected between metamorphic stages. Owing to the lack of statistical power in our analysis, we will focus our discussion only on groups of genes with distinct expression patterns between embryonic and early veliger stages in comparison to metamorphic stages (see Fig. 4 for definition of developmental phases).

Amino acids, neurotransmitters, low molecular weight, and water-soluble substances have frequently been shown to be directly or indirectly involved in signal transduction during settlement (reviewed in Heyland and Moroz, 2006). Many of these compounds function as modulators of the settlement process, but they likely act downstream of receptor activation. Among these neurotransmitters, 5-HT has been frequently suggested as a modulator of sensory input during settlement (reviewed in Heyland and Moroz, 2006). We find increased expression levels of genes related to 5-HT signaling at stage 6 (Figs. 2D and 3B–D), which is consistent with a function of 5-HT in metamorphic competence. In *Aplysia*, as in other molluscs, the ASO is lost and the adult ganglionic nervous system is becoming functional during metamorphosis (Diefenbach et al., '91; Couper and Leise, '96; Marois and Carew, '97a,b,c). Localization of serotonergic cells using both 5-HT antibody (Fig. 3C), and whole mount fluorescent in situ hybridization (WMISH) for gene products controlling 5-HT synthesis and transporter (Fig. 5), largely confirm previous studies and provide convincing evidence that the larval and adult nervous systems are separate structures (Marois and Carew, '97a,b,c).

Several transcripts coding for peptides are expressed at their highest level during metamorphic stages. This second group of transcripts, which is enriched in metamorphic stages, is related to the regulation of synapse structure and activity (Appendix 2; GO:0050803). As noted, the metamorphic transition is initiated by specific sensory signals and depends upon rearrangement of neuronal circuits. The establishment and modification of synapses is an important condition for associated behavioral changes. Interestingly, we also observed enrichment of transcripts encoding Ca^{2+} voltage-gated channels (e.g. the *Aplysia* homologs of P/Q-type calcium channel subunit α -1A (DA43656)) and Endophilin-A (DA2779), both of which may be involved in interneuronal and neuromuscular reorganization in metamorphic stages.

Three larval muscles in *Aplysia* degenerate in the process of settlement, whereas the buccal and anterior retractor muscles

differentiate during this process (Wollesen et al., 2008). We detected elevated expression of two specific regulators of myogenic differentiation in metamorphic stages. These are muscle LIM proteins (DA46517 and DA53418) and neural-type cell adhesion molecules (DA54034, a glycoprotein expressed at the surface of neurons and muscles). Furthermore, in the same cluster of metamorphosis-related transcripts, we identified titin (DA54287), a critical contributor to muscular contraction and ryanodine receptors (DA52090), known as intracellular calcium channels in both muscles and neurons (Zucchi and Ronca-Testoni, '97).

Metamorphic stages are also characterized by a marked change in metabolism that is in part related to the massive restructuring of the larva into a juvenile. Among several transcripts related to metabolic processes (see Appendix 2), we detected enrichment of two types of α -amylases (α -amylase 1 and 2; DA52041 and DA26218) in this category. These mRNAs are coding for enzymes that cleave α -bonds of large sugar molecules and, therefore, function in a wide diversity of metabolic processes in animals.

Transcriptional Changes Linked to Biomineralization. Molluscan biomineralization has been of broad scientific interest, ranging from paleontology (molluscan shells provide one of the best fossil records for a metazoan phylum) to material sciences (pearl and nacre formation). These disciplines have led to the identification of many putative shell-forming proteins. The organ involved in secreting shell proteins is the mantle, a specialized tissue layer that covers the visceral cavity and extends outwards in the form of flaps beyond the cavity itself. The shell is produced by a highly regulated process in the mantle that creates a composite biomaterial with a mineral phase of calcium carbonate (Addadi and Weiner, '92). This biomaterial accounts for 95–99% per weight of the shell, whereas the remaining 1–5% consists of the organic matrix (Addadi and Weiner, '92; Zhang and Zhang, 2006). This organic matrix controls different aspects of the shell formation processes, such as the synthesis of transient amorphous minerals and evolution to crystalline phases, the choice of the calcium carbonate polymorph (calcite vs. aragonite), and organization of crystallites in complex shell textures (microstructures) (Marin and Luquet, 2004; Marin et al., 2008). It is now known that one of the main components involved in the control of shell synthesis are the proteinaceous constituents of the shell matrix (Marin and Luquet, 2004; Marin et al., 2008).

In the *Aplysia* transcriptome, we identified 196 unique contigs coding for potential biomineralization genes (see Materials and Methods for details on annotation of the transcriptome and specifically the annotation of biomineralization genes). Next, we analyzed expression levels of these contigs throughout development and grouped them using cluster analysis (see Materials and Methods). Results are presented in Figure 6. Given that the shell becomes visible during the veliger stage, one would expect that

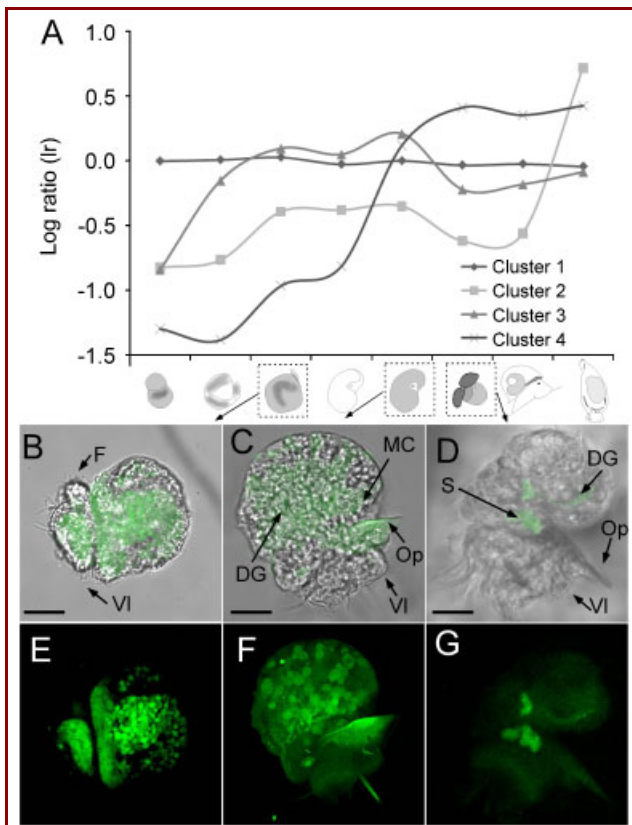


Figure 6. Transcription profiles of biomineralization genes. Using k-means cluster analysis, we were able to retrieve four distinct expression profiles of all annotated biomineralization genes (A). Clusters 2 and 4 represent contigs with elevated expression levels during metamorphic stages, Cluster 1 represents contigs that do not change their expression during development, and Cluster 3 represents contigs with elevated expression levels during trochophore and veliger stages. We analyzed gene expression of aragonite protein 24 (AP24) antisense probe, using whole mount fluorescent in situ hybridization (MWISH) on whole *A. californica* embryos and early larvae. Note that stages in Panel B–G are marked with a dashed box in panel A. Panels B–E, C–F, and D–G represent the same stages (trochophore, early veliger, and veliger stage 1, respectively B, E). The upper panel always shows the fluorescent image superimposed with the DIC image. Expression of AP24 is diffused throughout the trochophore larvae with high expression where the shell and operculum will be present. (C, F) Expression of AP24 within prehatching veliger. Some expression was detected in the operculum. (D, G) AP24 expression in posthatching stage 1 veligers is restricted to the statocyst and the digestive gland. AP24 is expressed during trochophore (A–B), prehatching early veliger stages (C–D), and posthatching stage 1 veligers (E–F), as predicted by the microarray data. F, foot; VI, velum lobes; Op, operculum; DG, digestive gland; S, statocyst; MC, mantle cells. Scale Bars: A: 35 μ m; C: 36 μ m; E: 34 μ m.

this stage marks the onset of biomineralization. However, the majority of biomineralization-related transcripts show little change in expression levels throughout the developmental stages assayed here (Fig. 6A; Cluster 1: 163 sequences). A closer look at the genes from Cluster 1 reveals that it contains many ribosomal genes. Ribosomal proteins are indispensable for protein biosynthesis, growth, and development, and hence we expect them to be constitutively expressed. Cluster 1 also contains many genes ($n = 71$) that were identified by Jackson et al. (2006), as expressed in the mantle secretome and did not yield BLAST-based annotations. As a consequence, we are not able to infer function for more than half of the genes in this cluster. The remainder of the genes from this cluster contains many genes that were identified to play a key role in shell construction and biomineralization in molluscs (e.g. N66 matrix protein (Zhang and Zhang, 2006), nacrein (Miyamoto et al., 2005), Pearlins (Kroger, 2009), and Perlucin (Mann et al., 2000)). Hence, genes that are essential in the biomineralization process of molluscs seem to be expressed constitutively during development, and not only in stages that coincide with the onset of biomineralization. Alternatively these genes could also be involved in more general functions thus their constitutive expression over time.

Cluster 2 (Fig. 6A) represents genes that are highly (> 20 fold) up-regulated 60 hr postmetamorphosis. This cluster contains three contigs that we annotated as a collagen α -1 chain (DA16646), agglutinin (DA19913) and dentin (DA21676). The function of these genes may be related to changes in shell composition and internalization, as *A. californica* internalizes its shell after settlement and reduces its size significantly. Cluster 3 (Fig. 6A) consists of 23 genes that show elevated expression levels during trochophore and veliger stages but not in metamorphic stages. Although not all 23 genes in this cluster could be annotated, we find several mantle genes as identified by Jackson et al. (2006) (DA13445, DA20577, DA20965, DA27225, DA36852, DA48551, DA51422). These transcripts represent interesting candidates for shell formation. Aragonite Protein 24 (AP24) groups within this cluster and is further discussed below. Finally, Cluster 4 (Fig. 6A) contains genes that show peptide-like expression profiles (i.e. low expression levels during early development and high expression levels late in development; see Fig. 7 and discussion below). This cluster contains a homolog of ferritin (DA20216), a mantle protein (DA48129), and the two neuropeptides, schistosomin (DA21974) and achatin (DA27773). Ferritins are multifunctional, multisubunit proteins that synthesize mineral precursors (Theil, 2003). In this respect, the continuous increase in expression from gastrulation to post-metamorphosis could pay tribute to an increased demand in biomineralization as a consequence of building the shell. The here-identified neuropeptides have so far not been functionally linked to the biomineralization process. However, the nature of our screening approach might give rise to genes that are not necessarily mechanistically linked to biomineralization; e.g. our

screen included all genes that were expressed in the mantle of *Haliotis anisina* (Jackson et al., 2006, 2007). Those genes do not necessarily need to play a role in biomineralization *per se*. It remains to be determined whether these neuropeptides may have acquired different developmental functions in *Aplysia* larvae or if their expression is correlated but not causally linked to biomineralization. Stage-specific WMISH of these genes could provide a first hint toward their role in biomineralization by highlighting their spatial expression.

AP24 (Cluster 3) was identified and isolated from the EDTA soluble matrix in the abalone *Haliotis refescens* (Michenfelder et al., 2003). Additionally, *in vitro* studies confirmed that AP24 is indeed a “true” shell-forming protein, and hence a constituent of the shell matrix. No WMISH have been performed for this gene to date. AP24 expression patterns follow those of cluster 3 (Fig. 6A), and WMISH of this gene in three developmental stages of *Aplysia* further provide data on the expression patterns of this gene. Specifically, we find AP24 to be highly expressed throughout the ectodermal tissue during early veliger stages, the site of the future mantle, and the velum and foot, adjacent to the future operculum in the trochophore larva (Fig. 6B and E). The expression patterns of AP24 in prehatching veligers are comparable to the trochophore stage with additional expression in the mantle tissue (Fig. 6C and F). Posthatching stage 1 veligers show restricted expression of AP24 in the ventral edge of the digestive gland and the statocyst (Fig. 6D and G).

Because the shell of *A. californica* does not contain any nacre, we hypothesize that this gene is involved in the secretion of aragonite crystals in *A. californica*. However, we also find expression of AP24 in regions that are not specific to shell formation, suggesting a broader function of this protein in biomineralization-related processes (Vue, unpublished data). Unfortunately, we were unable to get consistent expression patterns of genes that are expressed at relatively low levels during metamorphic stages. Therefore, we were unable to provide information on localization of AP24 expression during these stages. Our *in situ* protocol will require optimization for later larval stages when transcripts are less abundant (but see expression patterns for highly abundant pedal peptide; Fig. 7). Finally, negative controls (sense probe) were tested for all stages and resulted in no to negligible staining.

Endocrine and Neuroendocrine Signaling Pathways in *Aplysia* Development

A diversity of signaling mechanisms are employed during embryonic and larval development, and their use and composition can change drastically across stages. We analyzed the expression patterns of endocrine and neuroendocrine signal transduction in greater detail and discuss implications of our findings.

Secretory Products and Signal Peptides. From the 39,352 unique contigs, 204 contained signal peptide cleavage sites based on

SignalIP 3.0 server predictions (Bendtsen et al., 2004). A complete list of these predicted secretory products can be found in Appendix 2 column-Peps. We analyzed expression profiles of predicted secretory products using *k*-means cluster analysis and plotted the average gene expression levels from each of the four clusters (Fig. 7). In Figure 7A, average expression profiles of peptide clusters are plotted as a function of the developmental stage. Figure 7B shows selected candidate peptides and hormones from this group that were previously cloned from the CNS, and for which additional information is available (Moroz et al., 2006).

One general pattern that emerges from this dataset is the increase of expression levels as a function of developmental stage with a marked increase in metamorphic stages (Fig. 7B). Transcripts with a drastically different temporal expression pattern can be found in peptide Cluster 2 (Fig. 7A). Interestingly, the majority of these contigs could not be annotated at this point, and must therefore be specific to molluscs. One transcript from this cluster is a homolog of *Drosophila* papilin. Papilin is an extracellular matrix protein that has been shown to be essential for embryonic development in *D. melanogaster* and *C. elegans* (Fessler et al., 2004). The expression levels of *Aplysia* papilin are largely consistent with a function in embryogenesis. Further investigation of transcripts from this cluster may shed light on other essential components of embryonic development in *Aplysia*.

Genes from peptide Cluster 1 (Fig. 7A) show the strongest increase in expression levels correlated to developmental stage. This cluster contains several peptides, such as schistosomin, pedal peptide, and sensorin. Sensorin has been well characterized in *A. californica*, as it is expressed exclusively in mechanosensory neurons in the adult CNS (Walters et al., 2004). The dynamic expression pattern of these peptides suggests that they may be involved in regulating the metamorphic transition.

Cluster 3 generally consists of genes encoding predicted secretory products, which are expressed at low levels only during cleavage, and Cluster 4 contains predicted secretory peptide precursors and related enzymes that are highly expressed during metamorphic stages. Some of the genes from Cluster 4 can be generally assigned to intercellular signaling neuronal functions, such as neuroendocrine convertase (DA50171), neural cell adhesion molecule (DA36846), acetylcholine binding protein (DA22120), and Cysteine-rich motor neuron 2 protein (DA17080 and DA21546).

We tested spatial and temporal expression patterns of pedal peptide 1 (DA22082). This experiment served as a validation for our newly developed ISH protocol for *Aplysia* developmental stages, whereas at the same time providing insight into gene expression domains of this interesting peptide (Pearson and Lloyd, '89). Figure 7C–F shows tissue-specific mRNA localization of pedal peptide 1 using nonfluorescent ISHs in four different developmental stages. Temporal expression patterns for this gene were also analyzed using RT-PCR (Appendix 6) and suggest that pedal peptide 1 is highly expressed in larval and metamorphic

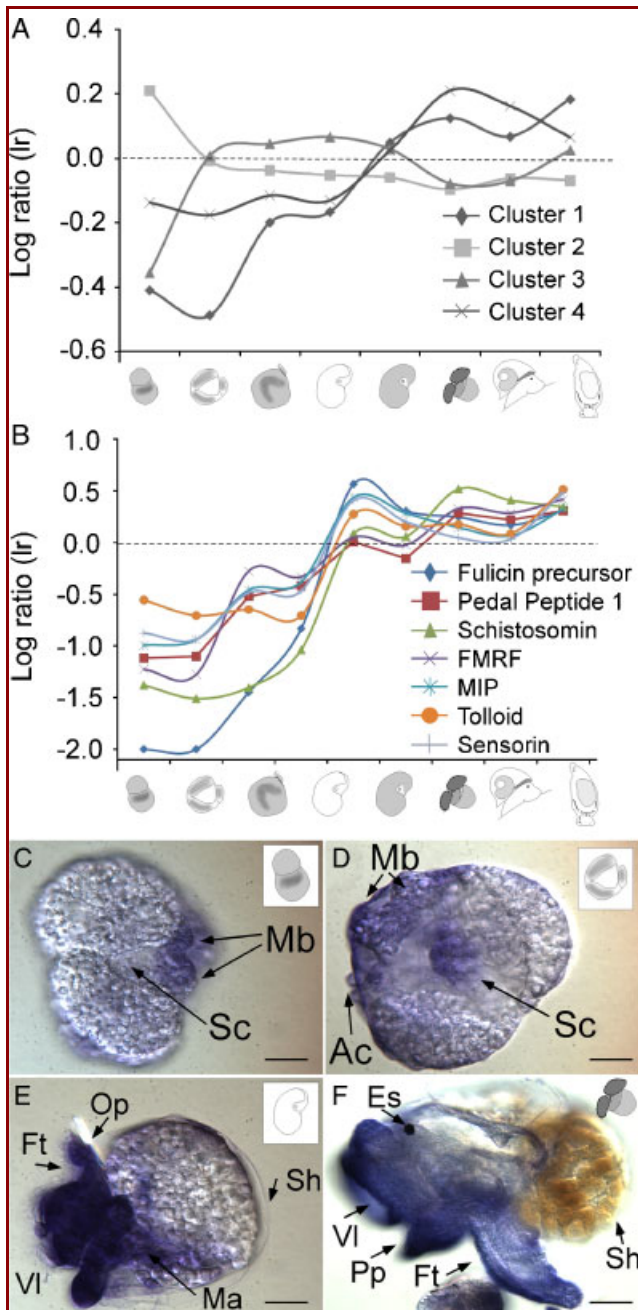


Figure 7. Transcription profiles of secretory products. We analyzed the expression patterns of 204 secretory products (i.e. contigs that show evidence for a signaling peptide sequence in any open reading frame; based on SignalP v.3.0 annotation, see Materials and Methods for details). Relative expression levels were grouped into four distinct clusters using k-means clustering algorithms and mean expression levels plotted as a function of time (A). Expression levels and details on individual contigs can be found in Appendix 2 column-Peps. Cluster 1 represents contigs that show very low

stages. Interestingly, the localization of the pedal peptide 1 mRNA is not limited only to the nervous system, but was also detected in the foot and velar lobe regions during metamorphic competence (Fig. 7F). Pedal peptide is known to be involved in control of locomotion and ciliated activity in molluscs (Hall and Lloyd, '90), and its observed expression pattern in foot and velar lobes of *Aplysia* veliger larvae is consistent with such predictions. Note that negative controls (sense probe) did not result in any specific staining pattern.

In addition to 5-HT, FMRF has been frequently used as a marker for the larval and juvenile nervous system of *A. californica*. Dickinson and Croll (2001) mapped cells with

Figure 7. (Continued) expression levels early in development and then increase and peak at metamorphic stages. We were also able to detect this pattern for selected neuropeptides which may play a role in larval development and nervous system patterning (see B). Cluster 2 represents contigs in which the expression levels are high early in development and then level out during larval and metamorphic stages. These secretory products may play a role in embryonic development. Note, however, that most of these secretory products could not be annotated. One notable exception is *papilin*, a matrix glycoprotein that is involved in gastrulation in *Drosophila melanogaster*. Secretory products from Cluster 3 were found at elevated levels during trochophore and early veliger stages inside the egg mass. This cluster also contains insulin-like growth factors which are further analyzed in Figure 7B. Cluster 4 represents genes that show slightly elevated expression levels during metamorphosis compared with embryonic development, but not as extreme as in Cluster 1. This cluster contains several peptides as well as other signaling molecules that have been shown to be involved in nervous system development. (B) We plotted expression profiles of seven selected neuropeptides for which we have full length clones in the lab and that have been characterized more extensively in our laboratories [A; GenBank accession numbers: Fulicin precursor (AAW30458.1), Pedal Peptide 1 (AAV84473.1), Schistosomin (AAV84471.1), FMRF (AAV41057), MIP (Q9NDE8.1), Tolloid (Q9Y6L7.1), Sensorin (P29233.1)]. The expression levels of all peptides increases posthatching and reaches maximum levels during the metamorphic transition. These peptides also show comparable expression patterns to Clusters 1 and 4 (A) and are consistent with the temporal dynamics of adult nervous system development inside the veliger larva (see Fig. 3). We used an antisense probe to further analyze expression patterns for pedal peptide 1 (C–F). We conclude that the diffuse staining in C and D is unspecific, based on the fact that it is not cell specific and significantly less intense compared with E and F. Consistently with the microarray data, we detected pedal peptide-1 at high levels in the foot and velar lobe region of veliger larvae posthatching (E) and at stage 6 (F; see Fig. 2 for staging information). A Scale bars: B: 18 μ m; C: 20 μ m; D: 50 μ m; E: 120 μ m. Mb, mesotoloblast cells.

FMRF-like immunoreactivity (FMRF-LIR) in *A. californica*. Their findings for peptide localization largely match with our microarray data detecting temporal mRNA levels for *Aplysia* FMRF (Fig. 7A). The first appearance of FMRF-LIR occurs pre-hatch in cells of the future adult ganglionic nervous system (Dickinson et al., 2000; Dickinson and Croll, 2001). FMRF-LIR expression levels then peak during metamorphic stages. These findings suggest a function of FMRF not only in embryonic behavior (Dickinson et al., 2000), but in patterning the adult nervous system as well.

Our data suggest that FMRF and pedal peptides are not the only signaling molecules modulating larval behavior during metamorphosis. In fact, more than 50% of all predicted secretory products (Clusters 1 and 4; Fig. 7) show comparable gene expression patterns to FMRF. Future studies identifying spatial gene expression patterns of these peptides will be instrumental in exploring the role of these signal molecules in life history transitions as well as in the larval and juvenile nervous systems.

Hormonal Signaling in Larval Development and Metamorphosis.

Hormonal signaling in larval development has been well investigated for holometabolous insects, frogs and some fish species, but for the majority of marine invertebrates we have little to no information on the significance of these important signaling pathways in development (Heyland et al., 2005). The larval body is a complex structure with a diversity of organ systems that needs to respond to a variety of environmental cues during larval development and the metamorphic transition (Heyland and Moroz, 2005). Hormonal signaling pathways have been previously discussed for *Aplysia* (Arch, '72; Chiu et al., '79; Rubakhin et al., '99; Pertseva and Shpakov, 2002; Gerencser et al., 2003; Thornton et al., 2003; Heyland and Moroz, 2005; Heyland et al., 2005, 2006; Moroz et al., 2006; Tsai et al., 2010), but no data exists to date on the involvement of hormonal regulation of development and, specifically, metamorphosis. Figure 8 shows the expression levels of several broad groups of signaling molecules that are associated with hormonal signal transduction cascades.

First, we analyzed expression patterns of 45 predicted hormone-signaling related genes, i.e. hormone activated proteins, hormone receptors and their ligands, hormone synthesis enzymes, enzymes related to hormone metabolism, and hormone binding protein. Expression profiles of six specific transcripts coding for such genes are plotted in Figure 8A. All these transcripts are relatively up-regulated in later developmental stages compared with embryonic stages; the individual patterns, however, are profoundly different. One interpretation of this general pattern is that these transcripts might be involved in the modulation of specific behaviors during the metamorphic transition, such as feeding and crawling (Fig. 3).

Hormone-like products represented in Figure 8A include two thyroid hormones- (THs) related transcripts (TH-induced protein: DA7089 and TH sulfotransferase: DA47476), cerebrin

(an *Aplysia* specific neuropeptide secreted from F-cluster cells in the central nervous system (Li et al., 2001) DA37072), bag cell egg-laying hormone (BCP; DA16715), a recently cloned new glycoprotein-like hormone (DA 37011), and a corticotropin-releasing factor binding protein (CRF-BP; DA42138). Functionally, these transcripts may be comparable to signal peptides and neuropeptides (discussed above), in that their release is linked to modulating feeding and crawling behavior during the metamorphic transition.

Insulins are conserved throughout the animal kingdom and one insulin type has been previously found to be expressed in the cerebral ganglion of adult *A. californica* (Floyd et al., '99). This gene seems to be highly expressed during early development of *Aplysia* (DA42444). Two insulin-like growth factor binding proteins (IGFBP-3; DA36214 and IGFBP-7; DA20244; Fig. 8B) also show relatively high expression levels during larval stages compared with embryonic stages.

The cytochrome P-450 (CYP) family is a large group of enzymes with functions related to steroid, drug, carcinogen, and mutagen metabolism (Hannemann et al., 2007). From 40 transcripts coding for CYPs, we were able to identify 3 that are differentially up-regulated during metamorphic competence only (Fig. 8C). In *D. melanogaster*, which uses ecdysone (20-hydroxyecdysone) as a metamorphic regulator, a superficially similar pattern was discovered (White et al., '99), and the authors hypothesized that regulation of CYP genes was linked to the synthesis of ecdysone premetamorphosis.

Steroid and THs signal through nuclear hormone receptors (NHRs) and we annotated 7 new NHRs in *A. californica*. The detailed results of this annotation can be found in Appendix 2. In Figure 8D, we plotted profiles of three NHRs as a function of developmental stage. Both NHR4 (DA9275) and NHR6 (DA13785) show elevated expression levels during cleavage stages compared with gastrulation. NHR6 expression levels then increase approximately five-fold, whereas expression levels of NHR4 are back to initial levels at metamorphosis. Expression levels of NHR7 (DA26161) are slightly higher during larval stages compared with cleavage stages (approximately two-fold). We recognized NHR4 as an ortholog to DR-78 (DA9275), NHR6 is orthologous to Vitamin D3 receptor (DA13785), and NHR7 is orthologous to HR96 (DA26161).

Comparison of Aplysia With Other Developmental Transcriptomes

This study was designed as a first step toward acquiring a larger scale perspective on gene expression patterns in *A. californica*, and correlates these patterns with morphological and physiological changes in the life history of the sea hare. *Aplysia* will have its genome sequenced and annotated in the future and in combination with our observations we can provide initial insights into putative gene functions during development. Here, we try to outline some general comparisons between the *Aplysia* transcriptome and similar studies in other organisms.

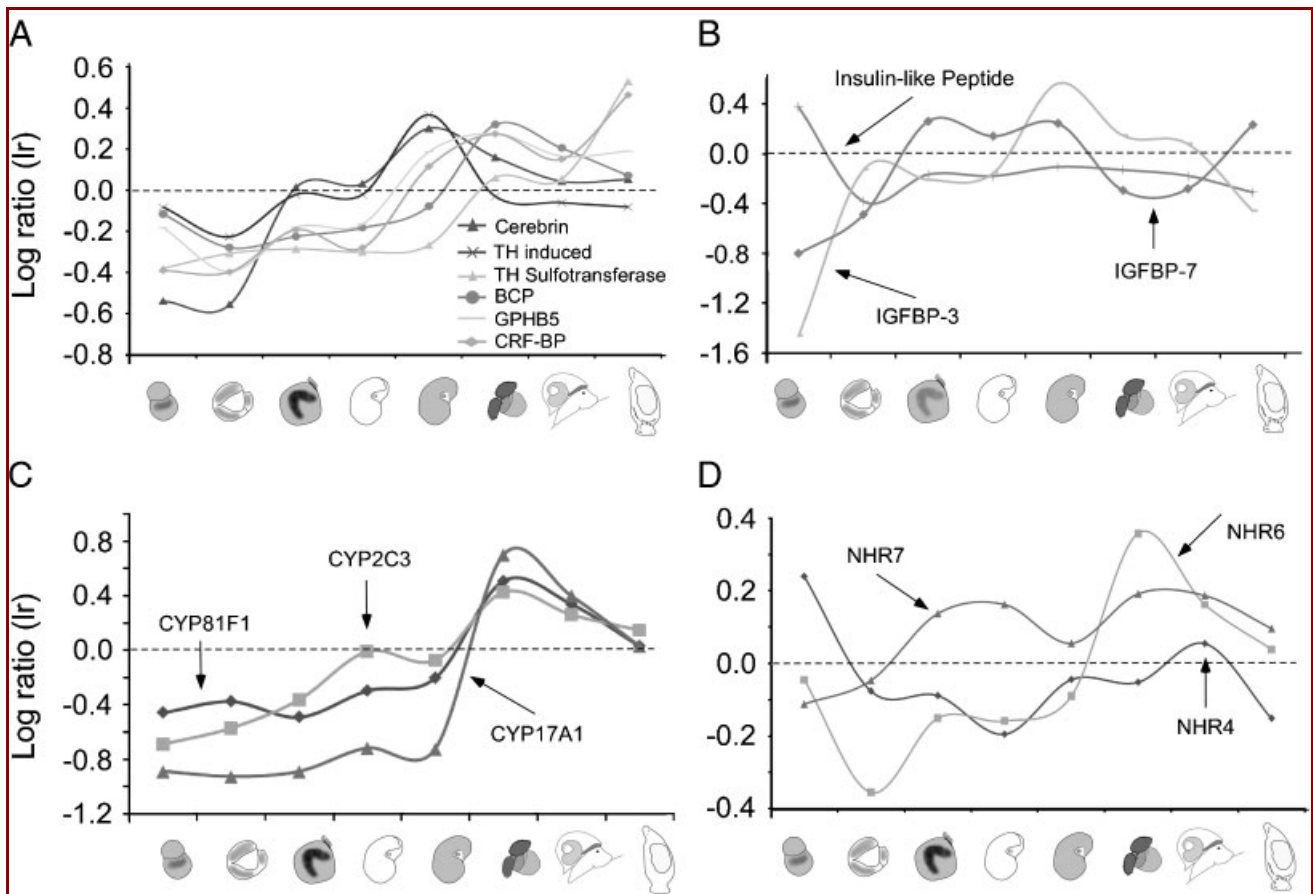


Figure 8. Transcriptional profiles of hormone-related genes. We analyzed expression profiles of groups of genes related to hormonal signaling pathways. (A) The majority of hormone-related transcripts follow a pattern of increased expression during larval and metamorphic stages. Several representatives are plotted here: Cerebrin (DA37072), thyroid hormone induced protein (DA7089), thyroid hormone sulfotransferase (DA47476), *Aplysia* bag cell peptide (BCP-DA16715), Thyrostimulin subunit (GPHB5-DA37011), and corticotrophin-releasing hormone binding protein (CRF-BP-DA42138). (B) We analyzed the expression of insulin-like peptides and insulin-like growth factors separately. Relative expression patterns of selected examples are: Insulin-like peptide (DA42444), Insulin-like growth factor binding protein 3 (IGFBP-3-DA36214), and Insulin-like growth factor binding protein 7 (IGFBP-7-DA20244). The cytochrome P-450 (CYP) family is a large group of enzymes with functions related to steroid, drug, carcinogen, and mutagen metabolism. From 40 transcripts coding for CYP, we were able to identify 3 that are differentially up-regulated during metamorphic competence only (C). Many hormones signal through nuclear hormone receptors. We annotated seven new NHRs from the *A. californica* transcriptome and plotted three of them in (D).

As outlined above, *Aplysia* larvae are metamorphically competent at stage 6 (Fig. 2D) and were induced to settle with algae as previously described (Kandel, '79). We find evidence for enrichment of the following GO categories in the metamorphically competent stage (Stage 6) compared with other larval stages (Fig. 4; Appendix 4): cell communication (GO:0007154), signal transduction (GO:0007165), enzyme regulator activity (GO:0030234), plasma membrane (GO:0005886), and receptor activity (GO:0004872). These categories contain more than 80 genes potentially involved in maintaining metamorphic competence in larvae. The analysis of these categories reveals that the

competent stage of veliger larvae (and potentially other larvae) is not static, with little to no gene transcription. Our analysis further shows that pre- and postmetamorphic stages seem to be very distinct (in terms of enriched GO categories). To further analyze the role of transcriptional regulation during the metamorphic transition, it would be necessary to perform a separate experiment that just focuses on developmental stages in the absence and presence of specific developmental cues. Williams et al. (2009) have provided an excellent example for such an experiment on the abalone *Haliotis asinina*. Still, some interesting similarities emerged from a preliminary comparison

of our results to the Williams et al. (2009) dataset. Soma ferritin is highly up-regulated during the metamorphic transition in both species. We also found a notable drop in expression levels of cyclophilin-A (DA30865) and HSP90 (DA21752) upon induction of settlement in *Aplysia*. Both these genes have been hypothesized to regulate the maintenance of metamorphic competence in *H. asinina*. A full list of differentially expressed transcripts shared between *H. asinina* and *A. californica* can be found in Appendix 2.

Fiedler et al. (2010) assessed absolute transcript levels of more than 7,000 *Aplysia* sequences using single pass sequencing analysis. We identified close to 4,000 sequences that matched specific contigs from our array database (for details, see Appendices 2 and 9). In Appendix 9, we compared the 15 most abundant transcripts by developmental stage between Fiedler et al. (2010) and this study. None of the comparisons revealed particularly similar patterns of gene expression. Further validation of this gene may be required to gain better insight into the transcriptional changes identified by Fiedler et al. (2010).

A recent study analyzed gene expression patterns during developmental stages of the zebrafish *D rerio* (Mathavan et al., 2005). We identified a group of 703 shared transcripts between this microarray analysis and ours, and compared expression levels during embryogenesis and nervous system formation between these two species (for a list of transcripts used in this analysis as well as details of comparison, see Appendix 8). Hierarchical cluster analysis using all zebrafish stages (unfertilized eggs, 3, 4.5, 6, 7.7, 9, 10, 12, and 15 hpf) and all *Aplysia* stages revealed little to no similarities of the global gene expression levels between these two species. Nevertheless, by comparing the expression levels of specific genes related to nervous system development and function, we identified some strong correlations. For example, neural cell adhesion molecule 1, tolloid-like protein 2, and Tryptophane-5 monooxygenase 1 expression are all critical for nervous system development, and their expression levels correlated strongly between *Aplysia* and zebrafish (Person's correlation coefficient >0.7). Dead-box protein 49, which shows relatively high expression levels early in development and low developmental levels late in development, was also strongly correlated between these two species (Person's correlation coefficient = 0.83). This gene was identified as a maternal transcript in zebrafish (Mathavan et al., 2005) and follows, therefore, a general pattern of decreased relative expression from early-to-late development. Interestingly, the cluster analysis including zebrafish and *Aplysia* expression levels revealed similarities between early cleavage stages of *Aplysia* and unfertilized eggs in zebrafish. Pearson correlation coefficients between these stages were significant and positive (PC = 0.135, $P < 0.001$; Appendix 8). These results can be interpreted as preliminary evidence for maternal gene expression in early cleavage and gastrula stages in *A. californica*.

Our analysis of the *Aplysia* transcriptome through development revealed a high percentage of homeobox-containing

transcripts enriched in larval stages and not in embryonic stages as expected (Appendix 2). Still, these findings confirm data by Von Stetina et al. (2007) from a developmental microarray analysis of the nematode *C. elegans*. As pointed out by Von Stetina et al. (2007), these findings can be explained by the fact that many transcripts are expressed in multiple cell types during embryogenesis and their expression then shifts toward neurons in larval stages (Von Stetina et al., 2007). Specifically, we were able to confirm POU (ceh-6) classes of homeodomain protein families, which are well established determinants of neuronal fate and are selectively enriched in both larvae of *C. elegans* and *Aplysia* (Appendix 2).

Several studies investigated large-scale transcriptional changes in the fruit fly *Drosophila melanogaster* and related species (White et al., '99; Arbeitman et al., 2002; Li and White, 2003; Rifkin et al., 2003). In *D. melanogaster*, a variety of behavioral changes occur in the process of metamorphosis, and similarly to *Aplysia*, these changes are correlated with drastic changes in neurosecretory status (White et al., '99; Li and White, 2003). Additionally, we were able to find differential expression of some plexin A genes during late larval development of *A. californica*. These genes are important players in axonal pathfinding and establishment of synaptic connections, and are differentially expressed during late larval stages in *D. melanogaster* as well (White et al., '99).

Intriguingly, *Drosophila* insulin that is expressed at higher levels during larval development seems to decrease in expression during the onset of metamorphosis, a pattern that is comparable to some insulin-like growth factor binding proteins we analyzed in *Aplysia*. In contrast to this, insulin-like peptide of *Aplysia* is up-regulated early in development. Studies on *Drosophila* have shown that *Drosophila* insulin is capable of stimulating proliferation and neural differentiation in the embryo (Pimentel et al., '96). Considering the early onset of neurons in *Aplysia*, such developmental function of insulin should be further investigated in the sea hare.

One microarray test on *D. melanogaster* identified major transcriptional changes during metamorphosis, related to the breakdown of larval muscles and adult myogenesis (White et al., '99). As in *Aplysia*, changes in gene expression of both structural and regulatory components as well as transcripts related to apoptosis are differentially expressed during this process. We found similarities in the expression patterns of apoptotic genes, which are further discussed in Appendix 2.

Although all these comparative data are preliminary, they raise interesting new questions about the involvement of endocrine- and neuroendocrine-signaling pathways in development that deserve further investigation. The mechanisms underlying the regulation of life history transition in marine invertebrate species is poorly understood and future work on *Aplysia* may help to elucidate them.

CONCLUSIONS

Our experiments provide novel insights into the dynamic mechanistic basis underlying *A. californica* development, metamorphosis, and neurogenesis. We have identified a broad scale of transcriptional changes that characterize different developmental stages, life history transitions, and molecular and cellular processes in *Aplysia*. mRNAs coding for neuropeptides are enriched in later developmental stages, a pattern that correlates with the development of the juvenile ganglionic nervous system and a transition from larval to adult body patterning. We also discovered several new *Aplysia* transcripts that are enriched in early cleavage stages, including regulators of chromatin remodeling and gene expression. Some of these genes can either be markers of early neurogenesis or might have been recruited for multiple divergent functions during development. Examples for such genes include transcription factors, which have been previously shown to be critical for *C. elegans* and *D. melanogaster* embryogenesis and neurogenesis. We also suggest that processes, such as hormonal signaling and peptide secretion, are predominantly active during metamorphosis in *Aplysia*, a finding that raises new questions about the regulation of life history transitions in animals. In addition to the molecular analysis of the metamorphic transition in *A. californica*, our study provides a starting point for future functional annotation of genome, given that *Aplysia* is a member of the largely understudied lophotrochozoan lineage. Hence, our study serves as a reference point that highlights the power of complementary analysis (molecular, morphological, and bioinformatical) in yielding insights into processes, such as development, biomineralization, and metamorphosis.

ACKNOWLEDGMENTS

This research was supported by the Swiss National Science Foundation Stipendium fuer Angehende Forscher and an NSERC-RGPIN (400230) and CFI grant (460175) to A.H. NIH (P50HG002806 and RO1NS06076, RR025699, DA030118), NSF (0744649), Brain Research Foundation grants to L.L.M., NSF grant (DEB-0542330) to M.M. We thank Tom Caprio from the University of Miami RSAS for providing us with various developmental stages of *Aplysia*. Shaikat Rangwala (MOGENE) provided invaluable help with the microarray experiments. Finally, we thank Drs. Detlev Arendt and Bernie Degnan for help with developing the in situ hybridization protocols for *A. californica*.

LITERATURE CITED

- Addadi L, Weiner S. 1992. Control and design principles in biological mineralization. *Angew Chem Int Ed Engl* 31:153–169.
- Andeol Y. 1994. Early transcription in different animal species—implication for transition from maternal to zygotic control in development. *Roux's Arch Dev Biol* 204:3–10.
- Arbeitman MN, Furlong EEM, Imam F, Johnson E, Hull BH, Baker BS, Krasnov MA, Scott MP, Davis RW, White KP. 2002. Gene expression during the life cycle of *Drosophila melanogaster*. *Science* 297:2270–2275.
- Arch S. 1972. Biosynthesis of egg-laying hormone (Elh) in bag cell neurons of *Aplysia californica*. *J Gen Physiol* 60:102–119.
- Bendtsen JD, Jensen LJ, Blom N, Von Heijne G, Brunak S. 2004. Feature-based prediction of non-classical and leaderless protein secretion. *Protein Eng Des Sel* 17:349–356.
- Blochmann F. 1883. Beitrage zur Kenntnis der Entwicklung der Gastropoden. *Z Wiss Zool* 38:392–410.
- Bluthgen N, Brand K, Cajavec B, Swat M, Herzog H, Beule D. 2005. Biological profiling of gene groups utilizing gene ontology. *Genome Inform* 16:106–115.
- Cai Y, Chia W, Yang X. 2001. A family of snail-related zinc finger proteins regulates two distinct and parallel mechanisms that mediate *Drosophila* neuroblast asymmetric divisions. *EMBO J* 20:1704–1714.
- Caprio TR, Bardales AT, Gillette PR, Lara MR, Schmale MC, Serafy JE. 2009. Larval growth, development, and survival of laboratory-reared *Aplysia californica*: effects of diet and veliger density. *Comp Biochem Physiol C Toxicol Pharmacol* 149:215–223.
- Chia FS, Rice ME. 1978. Settlement and metamorphosis of marine invertebrate larvae. New York: Elsevier. 290p.
- Chiu AY, Hunkapiller MW, Heller E, Stuart DK, Hood LE, Strumwasser F. 1979. Purification and primary structure of the neuropeptide egg-laying hormone of *Aplysia californica*. *Proc Natl Acad Sci USA* 76:6656–6660.
- Couper JM, Leise EM. 1996. Serotonin injections induce metamorphosis in larvae of the gastropod mollusc *Ilyanassa obsoleta*. *Biol Bull* 191:178–186.
- Davidson EH. 2001. Genomic regulatory systems: development and evolution. San Diego: Academic Press.
- Dickinson AJG, Croll RP. 2001. Neurocalcin-like immunoreactivity in embryonic stages of *Aplysia californica* and *Lymnaea stagnalis*. *Invertebr Biol* 120:206–216.
- Dickinson AJG, Croll RP, Voronezhskaya EE. 2000. Development of embryonic cells containing serotonin, catecholamines, and FMRFamide-related peptides in *Aplysia californica*. *Biol Bull* 199:305–315.
- Diefenbach TJ, Koehncke NK, Goldberg JL. 1991. Characterization and development of rotational behavior in *Helisoma* Embryos—role of endogenous serotonin. *J Neurobiol* 22:922–934.
- Fessler JH, Kramerova I, Kramerov A, Chen Y, Fessler LI. 2004. Papilin, a novel component of basement membranes, in relation to ADAMTS metalloproteases and ECM development. *Int J Biochem Cell Biol* 36:1079–1084.
- Fiedler TJ, Hudder A, McKay SJ, Shivkumar S, Caprio TR, Schmale MC, Walsh PJ. 2010. The transcriptome of the early life history stages of the California sea hare *Aplysia californica*. *Comp Biochem Physiol Part D Genom Proteom* 5:165–170.

- Floyd PD, Li L, Rubakhin SS, Sweedler JV, Horn CC, Kupfermann I, Alexeeva VY, Ellis TA, Dembrow NC, Weiss KR, Vilim FS. 1999. Insulin prohormone processing, distribution, and relation to metabolism in *Aplysia californica*. *J Neurosci* 19:7732–7741.
- Gerencser GA, Loo SY, Zhang J. 2003. Thyroid hormone-induced sulfate absorption in *Aplysia californica* gut is mediated by protein synthesis. *Can J Physiol Pharmacol* 81:405–408.
- Glanzman DL. 1995. The cellular basis of classical conditioning in *Aplysia californica*—it's less simple than you think. *Trends Neurosci* 18:30–36.
- Gotz S, Garcia-Gomez JM, Terol J, Williams TD, Nagaraj SH, Nueda MJ, Robles M, Talon M, Dopazo J, Conesa A. 2008. High-throughput functional annotation and data mining with the Blast2GO suite. *Nucleic Acids Res* 36:3420–3435.
- Hall JD, Lloyd PE. 1990. Involvement of pedal peptide in locomotion in *Aplysia*: modulation of foot muscle contractions. *J Neurobiol* 21:858–868.
- Hannemann F, Bichet A, Ewen KM, Bernhardt R. 2007. Cytochrome P450 systems—biological variations of electron transport chains. *Biochim Biophys Acta* 1770:330–344.
- He J, Dai X, Zhao X. 2007. PLAN: a web platform for automating high-throughput BLAST searches and for managing and mining results. *BMC Bioinform* 8:53.
- Heyland A, Moroz LL. 2005. Cross-kingdom hormonal signaling: an insight from thyroid hormone functions in marine larvae. *J Exp Biol* 208:4355–4361.
- Heyland A, Moroz LL. 2006. The signaling architecture underlying metamorphic transitions across animal phyla. *Integr Comp Biol* 46:743–759.
- Heyland A, Hodin J, Reitzel AM. 2005. Hormone signaling in evolution and development: a non-model system approach. *Bioessays* 27:64–75.
- Heyland A, Price DA, Bodnarova M, Moroz LL. 2006. Thyroid hormone metabolism and thyroid peroxidase function in two non-chordate animals. *J Exp Zool (Mol Dev Evol)* 306:551–566.
- Jackson DJ, McDougall C, Green K, Simpson F, Worheide G, Degnan BM. 2006. A rapidly evolving secretome builds and patterns a sea shell. *BMC Biol* 4:40.
- Jackson DJ, Worheide G, Degnan BM. 2007. Dynamic expression of ancient and novel molluscan shell genes during ecological transitions. *BMC Evol Biol* 7:160.
- Kandel ER. 1979. Behavioral biology of *Aplysia*: a contribution to the comparative study of opisthobranch molluscs. New York: Freeman.
- Kandel ER, Kriegstein A, Schacher S. 1980. Development of the central nervous system of *Aplysia* in terms of the differentiation of its specific identifiable cells. *Neuroscience* 5:2033–2063.
- Kempf SC, Page LR. 2005. Anti-tubulin labeling reveals ampullary neuron ciliary bundles in opisthobranch larvae and a new putative neural structure associated with the apical ganglion. *Biol Bull* 208:169–182.
- Kriegstein AR. 1977. Development of the nervous system of *Aplysia californica*. *Proc Natl Acad Sci USA* 74:375–378.
- Kriegstein AR, Castellucci V, Kandel ER. 1974. Metamorphosis of *Aplysia californica* in laboratory culture. *Proc Natl Acad Sci USA* 71:3654–3658.
- Kroger N. 2009. Biochemistry. The molecular basis of nacre formation. *Science* 325:1351–1352.
- Leonard JL, Edstrom JP. 2004. Parallel processing in an identified neural circuit: the *Aplysia californica* gill-withdrawal response model system. *Biol Rev Camb Philos Soc* 79:1–59.
- Li TR, White KP. 2003. Tissue-specific gene expression and ecdysone-regulated genomic networks in *Drosophila*. *Dev Cell* 5:59–72.
- Li L, Floyd PD, Rubakhin SS, Romanova EV, Jing J, Alexeeva VY, Dembrow NC, Weiss KR, Vilim FS, Sweedler JV. 2001. Cerebrin prohormone processing, distribution and action in *Aplysia californica*. *J Neurochem* 77:1569–1580.
- Linder P. 2000. Quick guide: DEAD-box proteins. *Curr Biol* 10:R887.
- Linder P. 2006. Dead-box proteins: a family affair: active and passive players in RNP-remodeling. *Nucleic Acids Res* 34:4168–4180.
- Livingston BT, Killian CE, Wilt F, Cameron A, Landrum MJ, Ermolaeva O, Sapojnikov V, Maglott DR, Buchanan AM, Etensohn CA. 2006. A genome-wide analysis of biomineralization-related proteins in the sea urchin *Strongylocentrotus purpuratus*. *Dev Biol* 300:335–348.
- Mackie GO, Singla CL, Thiriot-Quievreux C. 1976. Nervous control of ciliary activity in gastropod larvae. *Biol Bull* 151:182–199.
- Mann K, Weiss IM, Andre S, Gabius HJ, Fritz M. 2000. The amino-acid sequence of the abalone (*Haliotis laevis*) nacre protein perlucin. Detection of a functional C-type lectin domain with galactose/mannose specificity. *Eur J Biochem* 267:5257–5264.
- Marin F, Luquet G. 2004. Molluscan shell proteins. *Comptes Rendus Palevol* 3:469–492.
- Marin F, Luquet G, Marie B, Medakovic D. 2008. Molluscan shell proteins: primary structure, origin, and evolution. *Curr Top Dev Biol* 80:209–276.
- Marois R, Carew TJ. 1997a. Fine structure of the apical ganglion and its serotonergic cells in the larva of *Aplysia californica*. *Biol Bull* 192:388–398.
- Marois R, Carew TJ. 1997b. Ontogeny of serotonergic neurons in *Aplysia californica*. *J Comp Neurol* 386:477–490.
- Marois R, Carew TJ. 1997c. Projection patterns and target tissues of the serotonergic cells in larval *Aplysia californica*. *J Comp Neurol* 386:491–506.
- Mathavan S, Lee SG, Mak A, Miller LD, Murthy KR, Govindarajan KR, Tong Y, Wu YL, Lam SH, Yang H, Ruan Y, Korzh V, Gong Z, Liu ET, Lufkin T. 2005. Transcriptome analysis of zebrafish embryogenesis using microarrays. *PLoS Genet* 1:260–276.
- Melkonyan HS, Chang WC, Shapiro JP, Mahadevappa M, Fitzpatrick PA, Kiefer MC, Tomei LD, Umansky SR. 1997. SARPs: a family of secreted apoptosis-related proteins. *Proc Natl Acad Sci USA* 94:13636–13641.
- Michenfelder M, Fu G, Lawrence C, Weaver JC, Wustman BA, Taranto L, Evans JS, Morse DE. 2003. Characterization of two molluscan crystal-modulating biomineralization proteins and

- identification of putative mineral binding domains. *Biopolymers* 70: 522–533.
- Miyamoto H, Miyoshi F, Kohno J. 2005. The carbonic anhydrase domain protein nacrein is expressed in the epithelial cells of the mantle and acts as a negative regulator in calcification in the mollusc *Pinctada fucata*. *Zool Sci* 22:311–315.
- Moroz LL, Ju J, Russo JJ, Puthanveetti S, Kohn A, Medina M, Walsh PJ, Birren B, Lander ES, Kandel ER. 2004. Sequencing the *Aplysia* genome: a model for single cell, real-time and comparative genomics. (National Human Genome Research Institute online at <http://www.genome.gov/Pages/Research/Sequencing/SeqProposals/AplysiaSeq.pdf>.)
- Moroz LL, Edwards JR, Puthanveettil SV, Kohn AB, Ha T, Heyland A, Knudsen B, Sahni A, Yu F, Liu L, Jezzini S, Lovell P, Iannuccilli W, Chen M, Nguyen T, Sheng H, Shaw R, Kalachikov S, Panchin YV, Farmerie W, Russo JJ, Ju J, Kandel ER. 2006. Neuronal transcriptome of *Aplysia*: neuronal compartments and circuitry. *Cell* 127:1453–1467.
- Nielsen KK, Nielsen JE, Madrid SM, Mikkelsen JD. 1997. Characterization of a new antifungal chitin-binding peptide from sugar beet leaves. *Plant Physiol* 113:83–91.
- Page LR. 2002. Comparative structure of the larval apical sensory organ in gastropods and hypotheses about function and developmental evolution. *Invertebr Reprod Dev* 41:193–200.
- Page LR. 2003. Gastropod ontogenetic torsion: developmental remnants of an ancient evolutionary change in body plan. *J Exp Zool (Mol Dev Evol)* 297:11–26.
- Panchin YV. 2005. Evolution of gap junction proteins: the pannexin alternative. *J Exp Biol* 208:1415–1419.
- Pearson WL, Lloyd PE. 1989. Immunocytochemical localization of pedal peptide in the central nervous system and periphery of *Aplysia*. *J Neurosci* 9:318–325.
- Pertseva MN, Shpakov AO. 2002. Conservatism of the insulin signaling system in evolution of invertebrate and vertebrate animals. *J Evol Biochem Physiol* 38:547–561.
- Pimentel B, de la Rosa EJ, de Pablo F. 1996. Insulin acts as an embryonic growth factor for *Drosophila* neural cells. *Biochem Biophys Res Commun* 226:855–861.
- Rassart E, Bedirian A, Do Carmo S, Guinard O, Sirois J, Terrisse L, Milne R. 2000. Apolipoprotein D. *Biochim Biophys Acta* 1482: 185–198.
- Ren M, Drivas G, D'Eustachio P, Rush MG. 1993. Ran/TC4: a small nuclear GTP-binding protein that regulates DNA synthesis. *J Cell Biol* 120:313–323.
- Rifkin SA, Kim J, White KP. 2003. Evolution of gene expression in the *Drosophila melanogaster* subgroup. *Nat Genet* 33:138–144.
- Robb SM, Ross E, Sanchez Alvarado A. 2008. SmedGD: the *Schmidtea mediterranea* genome database. *Nucleic Acids Res* 36: D599–D606.
- Rubakhin SS, Li L, Moroz TP, Sweedler JV. 1999. Characterization of the *Aplysia californica* cerebral ganglion F cluster. *J Neurophysiol* 81:1251–1260.
- Suarez-Castillo EC, Garcia-Ararras JE. 2007. Molecular evolution of the ependymin protein family: a necessary update. *BMC Evol Biol* 7:23.
- Theil EC. 2003. Ferritin: at the crossroads of iron and oxygen metabolism. *J Nutr* 133:1549S–1553S.
- Thornton JW, Need E, Crews D. 2003. Resurrecting the ancestral steroid receptor: ancient origin of estrogen signaling. *Science* 301: 1714–1717.
- Tsai PS, Sun B, Rochester JR, Wayne NL. 2010. Gonadotropin-releasing hormone-like molecule is not an acute reproductive activator in the gastropod, *Aplysia californica*. *Gen Comp Endocrinol* 166: 280–288.
- Von Stetina SE, Watson JD, Fox RM, Olszewski KL, Spencer WC, Roy PJ, Miller 3rd DM. 2007. Cell-specific microarray profiling experiments reveal a comprehensive picture of gene expression in the *C. elegans* nervous system. *Genome Biol* 8:R135.
- Walters ET, Bodnarova M, Billy AJ, Dulin MF, Diaz-Rios M, Miller MW, Moroz LL. 2004. Somatotopic organization and functional properties of mechanosensory neurons expressing sensorin—a mRNA in *Aplysia californica*. *J Comp Neurol* 471:219–240.
- White KP, Rifkin SA, Hurban P, Hogness DS. 1999. Microarray analysis of *Drosophila* development during metamorphosis. *Science* 286: 2179–2184.
- Wilkins AS. 2001. The evolution of developmental pathways. Sunderland, MA: Sinauer Associates, Inc.
- Williams EA, Degnan BM, Gunter H, Jackson DJ, Woodcroft BJ, Degnan SM. 2009. Widespread transcriptional changes pre-empt the critical pelagic-benthic transition in the vetigastropod *Haliotis asinina*. *Mol Ecol* 18:1006–1025.
- Wollesen T, Wanninger A, Klussmann-Kolb A. 2007. Neurogenesis of cephalic sensory organs of *Aplysia californica*. *Cell Tissue Res* 330: 361–379.
- Wollesen T, Wanninger A, Klussmann-Kolb A. 2008. Myogenesis in *Aplysia californica* (Cooper, 1863) (Mollusca, Gastropoda, Opisthobranchia) with special focus on muscular remodeling during metamorphosis. *J Morphol* 269:776–789.
- Zhang C, Zhang R. 2006. Matrix proteins in outer shells of molluscs. *Mar Biotechnol* 8:572–586.
- Zucchi R, Ronca-Testoni S. 1997. The sarcoplasmic reticulum Ca²⁺ channel/ryanodine receptor: modulation by endogenous effectors, drugs and disease states. *Pharmacol Rev* 49:1.51.